AD 737 350

STRUCTURAL FLIGHT TEST OF AN AC-130A GUNSHIP EMPENNAGE

by

CAPTAIN JOHN J. RUSSELL

RESEARCH REPORT 71-9

OCTOBER 1971

UNITED STATES AIR FORCE ACADEMY

COLORADO 80840

UNCLASSIFIED

Security Classification

DOCUMENT CONTROL DATA - R & D

(Security classification of title, body of abstract and indexing annotation must be entered when the overall report is classified)

1. ORIGINATING ACTIVITY (Corporate author) Dean of Faculty USAF Academy, Colorado 80840	2a. REPORT SECURITY CLASSIFICATION UNCLASSIFIED 2b. GROUP

3. REPORT TITLE

STRUCTURAL FLIGHT TEST OF AN AC-130A GUNSHIP EMPENNAGE

4. DESCRIPTIVE NOTES (Type of report and inclusive dates)

Research Report

5. AUTHOR(S) (First name, middle initial, last name)

Captain John J. Russell

6. REPORT DATE	7a. TOTAL NO. OF PAGES	7b. NO. OF REFS
October 1971	64	0

8a. CONTRACT OR GRANT NO	9a. ORIGINATOR'S REPORT NUMBER(S)
b. PROJECT NO.	RR 71-9
c.	9b. OTHER REPORT NO(S) (Any other numbers that may be assigned this report)
d.	NONE

10. DISTRIBUTION STATEMENT

Distribution of this document is unlimited

11. SUPPLEMENTARY NOTES	12. SPONSORING MILITARY ACTIVITY
	Dean of Faculty USAF Academy, Colorado 80840

13. ABSTRACT

An AC-130A aircraft empennage was instrumented with electrical-resistance strain gages and flight test data was obtained for antiaircraft evasive maneuvers, 20mm General Electric Vulcan cannon firings, and 40mm Bofors gun firings. Complete descriptions of the test instrumentation, test conditions, strain gage locations, and results are contained in the report. Strain gages were located in the aircraft empennage area based on minimum margins of safety as found in the original Lockheed stress analysis. Results show that those stresses caused by gun firing, either 20mm or 40mm, are quite small and that the sum of the stresses due to the left hand orbit maneuver and the gun firing is well below design limits. Stresses produced by antiaircraft evasive maneuvers were also found to be well below design limits.

DD FORM 1 NOV 65 1473

UNCLASSIFIED

Security Classification

STRUCTURAL FLIGHT TEST OF AN AC-130A GUNSHIP EMPENNAGE

by

Captain John J. Russell

UNITED STATES AIR FORCE ACADEMY

RESEARCH REPORT 71-9

OCTOBER 1971

The research reported in this document was made possible in part by support extended to the faculty of the United States Air Force Academy by the Air Force Systems Command.

Additional copies of this document may be obtained by writing to the Director of Faculty Administration, United States Air Force Academy, Colorado 80840.

Editorial Review by Captain John B. McTasney
Department of English

This Research Report is presented as a competent treatment of the subject, worthy of publication. The United States Air Force Academy vouches for the quality of the research, without necessarily endorsing the opinions and conclusions of the authors.

TABLE OF CONTENTS

		Page
	Abstract	v
	List of Figures	vi
	List of Tables	viii
	List of Symbols	ix
I.	Introduction	1
	Improved Theoretical Stress Analysis	1
	New Actual Stress Analysis	1
II.	Instrumentation	3
	Strain Gages	3
	Temperature Compensation	4
	Bridge Balance Units	5
	Recorder	5
	Power Supply	5
III.	Aircraft Area Tested	5
	Strain Gage Location	7
	Vertical Stabilizer Gages	7
	Aft Fuselage Gages	9
	Gun Mount Gages	12
IV.	Flight Test	13
	Pre-flight	13
	In-flight	13
	Post-flight	13
V.	Results	14
	Calculations	14
	Level Flight Stresses	15
	Gun Firing Stresses	15
	Evasive Maneuver Stresses	15

VI. Conclusions and Recommendations 16
VII. List of References . . . . [illegible]
VIII. Appendix 21

ABSTRACT

An AC-130A aircraft empennage was instrumented with electrical-resistance strain gages and flight test data was obtained for anti-aircraft evasive maneuvers, 20mm General Electric Vulcan cannon firings, and 40mm Bofors gun firings. Complete descriptions of the test instrumentation, test conditions, strain gage locations, and results are contained in the report. Strain gages were located in the aircraft empennage area based on minimum margins of safety as found in the original Lockheed stress analysis. Results show that those stresses caused by gun firing, either 20mm or 40mm, are quite small and that the sum of the stresses due to the left hand orbit maneuver and the gun firing is well below design limits. Stresses produced by antiaircraft evasive maneuvers were also found to be well below design limits.

LIST OF FIGURES

Figure		Page
1	Overall Equipment Schematic	2
2	Wheatstone Bridge Schematic	4
3	AC-130 Aircraft Station Diagram	6
4	Vertical Stabilizer Structure	8
5	Aft Fuselage Structure FS 737 to FS 869	10
6	Aft Fuselage Structure FS 869 to FS 1041	11
7	Number 4 - 40mm Gun	12
8	Vertical Stabilizer - Main Beam	23
9	Vertical Stabilizer - Auxiliary Beam	23
10	Vertical Stabilizer - Rear Beam	24
11	Fuselage Station 814 Frame	25
12	Fuselage Station 847 Canted Bulkhead Installation	26
13	Fuselage Station 990 Frame	27
14	Upper BL 61 Longeron Fitting Fuselage Station 737 Fwd and Longeron	28
15	Lower B6 61 Longeron Fuselage Station 737 Aft	28
16	Upper BL 61 Longeron Fitting Fuselage Station 1041.5	29
17	Upper B6 61 Longeron Section at Fuselage Station 992	29
18	Upper B6 61 Longeron Section at Fuselage Station 1020	29
19	Lower B6 61 Longeron Fitting at Fuselage Station 1041.5 Fwd.	30
20	Lower Bl 61 Longeron Section at Fuselage Station 1030	30
21	Upper Dorsal Longeron Fitting at Fuselage Station 946	31
22	Aft Fuselage Skins and Splices	32
23	Definition of Symbols in Tables III and IV	33
24	Typical Trace .40mm. Gages Gl and G2	34
25	Typical Trace .40mm. Gage AF13	34
26	Typical Trace .40mm. Rosette Gage VS4R	35
27	Typical Trace .40mm. Gage VS6	35

28 Typical Trace .40mm. Rosette Gage AF21R 36
29 Typical Trace .40mm. Gage AF10 36
30 Typical Trace .20mm. Rosette Gage AF21R 37
31 Typical Trace .20mm. Gage AF10 37
32 Typical Traces - Antiaircraft Evasive Maneuvers 38

LIST OF TABLES

Table Page

I Summary of Vertical Stabilizer Strain Gage Locations 39

II Summary of Aft Fuselage and Gun Strain Gage Locations . . . 41

III Experimental Stresses Vertical Stabilizer 43

IV Experimental Stresses Aft Fuselage and Gun 45

LIST OF SYMBOLS

$\Delta\sigma_{LF}$ = Change in stress from installation stress to level flight stress.

$\Delta\sigma_{o}$ = Change in stress from installation stress to left hand orbit stress.

$\Delta\sigma_{+}$ = Change in stress from left hand orbit stress to positive peak of gun fire stress.

$\Delta\sigma_{-}$ = Change in stress from left hand orbit stress to negative peak of gun fire stress.

$\Delta\sigma_{max}$ = Change in stress from installation stress to positive peak of gun fire stress or positive peak of antiaircraft evasive maneuver stress.

$\Delta\sigma_{min}$ = Change in stress from installation stress to negative peak of gun fire stress or negative peak of antiaircraft evasive maneuver stress.

VS9 = Sample linear gage designation (Vertical Stabilizer 9).

VS10R = Sample rosette gage designation (Vertical Stabilizer 10 Rosette).

NOTE: These stresses are normal stresses when associated with linear gages and shear stresses when associated with rosette gages.

STRUCTURAL FLIGHT TEST OF AN AC-130A
GUNSHIP EMPENNAGE

Several operations separate the AC-130A gunship from its transport counterpart, the C-130A. Although loads imposed by the assault landings on transport aircraft cause more severe landing stresses than those encountered in gunship operations, side firing weapons impose loads on the gunship similar to lateral gusts, but with a much higher frequency of occurrence. Evasive maneuvers to avoid antiaircraft fire also impose unusual loads on gunships directly related to the severity of the gunfire. Therefore, while both transport and gunship versions use the same airframe, their operational environments are quite different.

Improved Theoretical Stress Analysis

Improvements in theoretical stress analysis techniques make the original stress analysis obsolete, although newer analysis techniques usually prove the older analysis to be conservative. Static tests have shown some of the assumptions in the original analysis to be incorrect, and appropriate modifications to the analysis were made. Therefore, while the tests show the theoretical analysis adequate for normal operations, they have not demonstrated the same adequacy for gunship operations.

New Actual Stress Analysis

Since a new stress analysis was not conducted for the AC-130A, gunship configuration, an experimental flight test investigation of stresses imposed by gunfiring and antiaircraft evasive maneuvers was conducted, not only to determine possible trouble areas (or conversely to determine their nonexistence), but also to extend gunship technology in the area of structural requirements criteria. The test results would also yield guide lines for the selection of a larger weapons system for follow on programs.

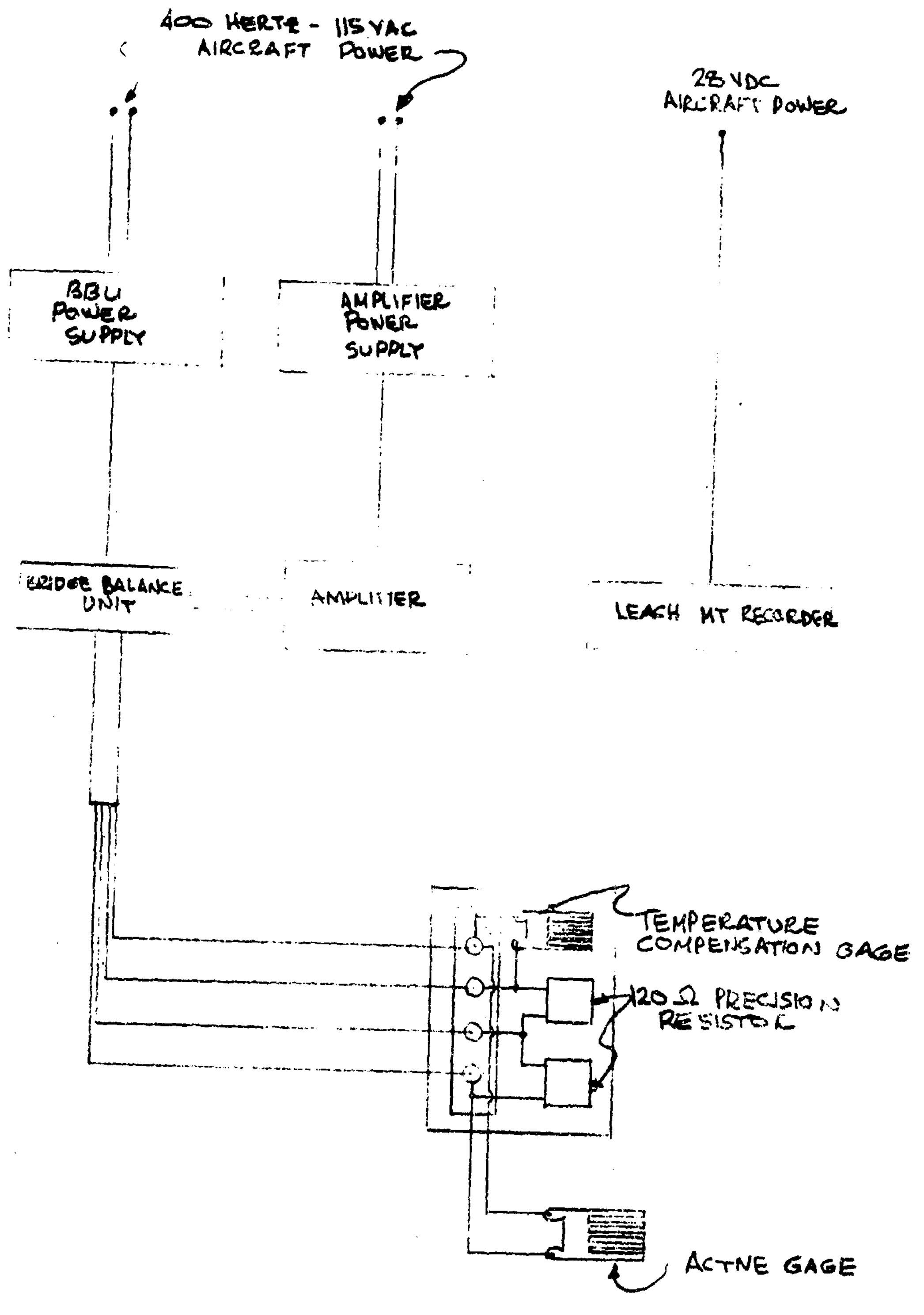

FIG. 1 OVERALL EQUIPMENT SCHEMATIC

INSTRUMENTATION

A complete schematic of the instrumentation package used in the test is shown in Figure 1 on the facing page. A standard Wheatstone bridge circuit, using a parallel bridge balance and a calibration resistor, was employed (See Figure 2). Automation Industries C12-121 were used for all linear gage applications, while C12-122D-R3Y were used for all rosette applications. A gage of the same type as the active gage was used as the temperature compensating gage in all cases.

Strain gages. Electrical resistance strain gages were selected as the transducers or the test because they possess the following advantages:

1. Direct strain indication at a selected point.
2. No need for theoretical calculations to obtain desired results; therefore, a direct comparison may be made between the measured strain and that predicted by the theoretical stress analysis.
3. High reliability for short term tests without elaborate installation procedures.
4. Continuous dynamic output; therefore, yielding frequency as well as amplitude data.

Two types of gages were used in the test, linear, and delta rosette. Linear gages capable of measuring only uniaxial strain were employed wherever the direction of principal strain was known, as in members which are loaded axially or in bending. Delta rosettes, three linear gages arranged at 120 degree spacing, were used when the direction of principal strains were unknown, such as for semi-tension shear panels and fuselage skin. Eleven linear and five rosette gages were utilized on the vertical stabilizer. Fourteen linear and three rosette gages were used to study aft fuselage stresses. In addition, two linear gages were placed on the 40mm gun mount such that present test data could be correlated with the results of a test conducted at Fort Carson, Colorado in August, 1970. In that test a 40mm gun mount was fully instrumented

with strain gages to determine how gunfiring loads were transmitted by the mount to the aircraft.

Temperature compensation. The temperature compensating gage and two 120 ohm precision resistors used to complete the bridge were fixed to an aluminum or steel block, depending upon the parent material of the active gage (See Figure 2). The block was then located as close as possible to the active gage, using a non-strain transferring adhesive to bond the block to the aircraft. The dummy block was placed near the active gage to complete the bridge circuit at the active gage, therefore obtaining both temperature compensation and common mode rejection.*

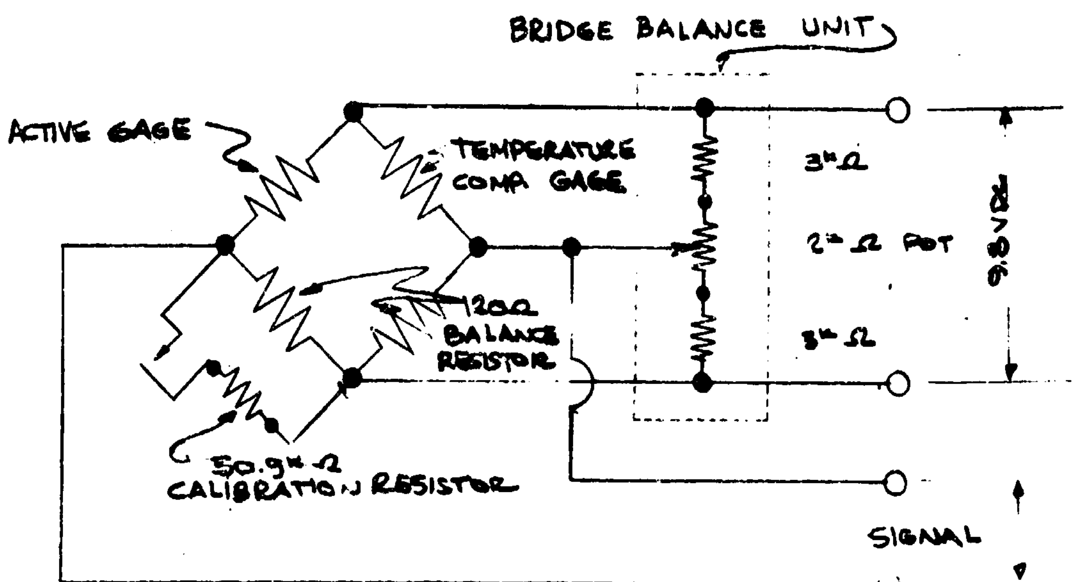

FIG2 Wheatstone Bridge Schematic

*Common mode rejection is the ability of the circuit to eliminate noise which appears on pairs of input lines by means of cancellation. This is accomplished in this circuit by having equal length lines leading to the gage and returning from the bridge such that the same noise is picked up by each pair of the wires returning the signal to the amplifiers. Since a differential amplifier was used, signals common to both lines are eliminated, thus obtaining common mode rejection.

Bridge balance units. The balancing circuits and calibration resistor (See Figure 2) were contained in the bridge balance units (BBU). Four BBU's with 12 channel capability and one BBU with ten channel capability were used in the test system, allowing for 58 channels of data. The calibration resistor was chosen to obtain a simulated strain of -1869 microstrain. Therefore, when the calibration resistor was switched into the circuit, a signal was generated equivalent to the signal of an 1869 microstrain compression load.

Recorder. A Leach Model MTR 3240 recorder with 14 channel data capability was used to record all the strain data. Since the output of only one BBU could be recorded at anytime, only 12 channels of the recorder were used. The data was recorded at a tape speed of 30 inches per second.

Power supply. Two power supplies were employed: one supplied 9.8 VDC to the strain gage network and the other supplied power to the amplifiers. Both were supplied by 115 VAC, 400 hertz aircraft power. Standard 28 VDC aircraft power was used for the tape recorder. The strain gage power supply exhibited a breakdown in the AC-DC conversion and started passing a 400 hertz ripple at a very low voltage causing some problems.

AIRCRAFT AREA TESTED

The empennage area of the aircraft was selected for the test because it was thought that most of the force resisting gun recoil would be provided by the vertical stabilizer. These forces could, therefore, produce a large gust type loading on the vertical stabilizer and a large torsional load on the aft fuselage. This area was also considered a potential trouble spot because all gunships fly with the rear cargo door open creating an open cross-section which is structurally inefficient for carrying torsional loads.

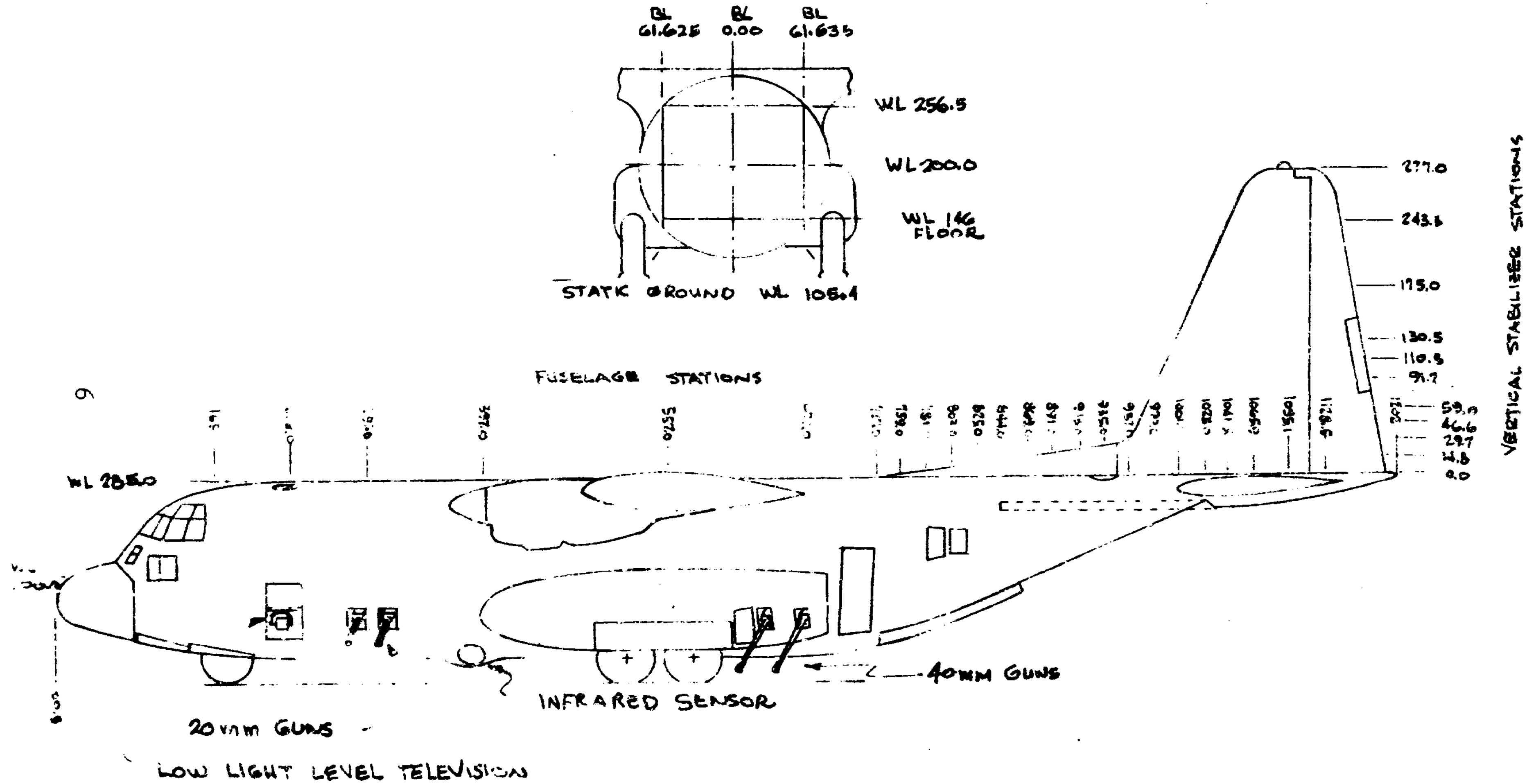

FIG. 3 AC-130 AIRCRAFT STATION DIAGRAM

The critical design conditions for the empennage were 1) asymmetrical power, 2) 15 psi fuselage pressurization, 3) maneuver loading, 4) lateral gust, and 5) hard rudder kick. While the lateral gust condition most closely simulates gunfiring loads, the dominant design condition for the empennage structure was the asymmetric condition.

The empennage, especially the vertical stabilizer, does not carry large dead weight loads. Hence, when the strain gages were installed, the empennage was in a zero stress condition. Even if this were not true, a great deal of information on over-stresses due to gunfiring and evasive maneuvers could be obtained, although the magnitude of the total stress could not be used. All stresses in this report will be referred to as changes in stress from the installation zero stress.

Strain Gage Locations

Strain gages were placed at points in the aft fuselage and vertical stabilizer with minimum margins of safety, based on References 1 and 2 in the List of References. Figure 3, page 6, provides fuselage station (FS), water line (WL), buttock line (BL), and vertical stabilizer station (VSS) information to aid in the general location of each gage. Locations of sensors, 20mm guns, and 40mm guns in relation to the gages may also be obtained from Figure 3. All gages were located aft of FS 737.

Vertical stabilizer gages (VS). Only the main load carrying members of the vertical stabilizer were instrumented. Figure 4, page 8, illustrates the general structural configuration of the vertical stabilizer, the main load carrying members being the auxiliary beam, main beam, and rear beam. All of these members were designed as semitension field beams. No gages were employed on the vertical stabilizer leading edge. Figure 4 also aids in finding the general location of all vertical stabilizer gages. Figures 8, 9, and 10 (Appendix) show the exact location of each gage on the auxiliary, main, and rear beams.

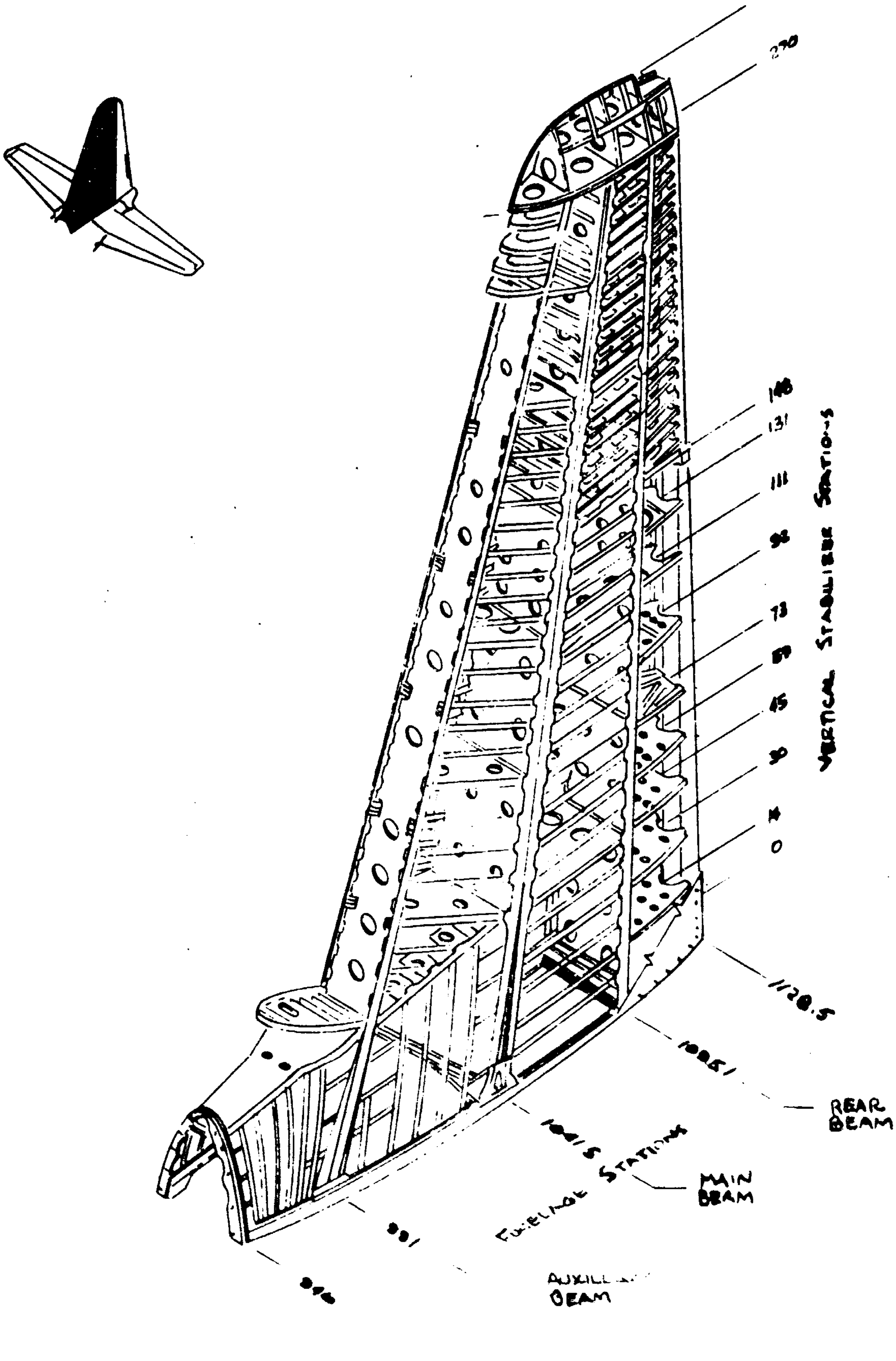

FIG. 4 VERTICAL STABILIZER STRUCTURE

The structural members instrumented were beam caps (VS5), stiffeners (VS3, VS6, VS14, VS14A, VS17), shear webs (VS4R, VS7R, VS8R, VS13R, VS18R) and fittings (VS9, VS10, VS19, VS20). Some gages were used only as checks on loads to insure the loads were below design levels. The check gages are noted in Table I (Appendix), which is a summary of vertical stabilizer strain gage locations, with additional information as to the critical design condition for each part, type of stress, and margin of safety.

Aft fuselage gages (AF). Figures 5 and 6, following, illustrate the aft fuselage internal structure. As in the vertical stabilizer only primary structure was instrumented. The basic fuselage structure is essentially a single cell thin walled tube (the aircraft skin) supported by transverse frames or rings as well as symmetrically arranged longerons. The skin carries only a shear load, while the frames carry combined axial and bending loads. The C-130 utilizes only four longerons arranged symmetrically at upper and lower BL 61.625.

Frames instrumented were at FS814 (AF4, AF5)(See Figure 11), FS 847 (AF6)(See Figure 12), FS 990 (AF1, AF3)(See Figure 13.) The longerons at upper and lower BL 61.625 were extensively instrumented, with gages being located at splice fittings or at critical locations as shown in Figures 14, 15, 16, 17, 18, 19 and 20 (AF7, AF8, AF10, AF11, AF12, AF13, AF14, AF15)(See Appendix). Gage AF18 was located on the upper dorsal longeron fitting as shown in Figure 21 (Appendix). The dorsal fin provides the fuselage with a second structural cell to add extra strength where the fuselage corss-section is open (due to the cargo door being open.) Three rosettes were placed on the fuselage skin (AF20R, AF21R, AF22R) as shown in Figure 22 (Appendix).

Table II (Appendix) provides summary information on all aft fuselage gages. Since the cargo ramp, aft cargo door, and horizontal stabilizer carry no unusual loads unique to gunship operations, they were not instrumented.

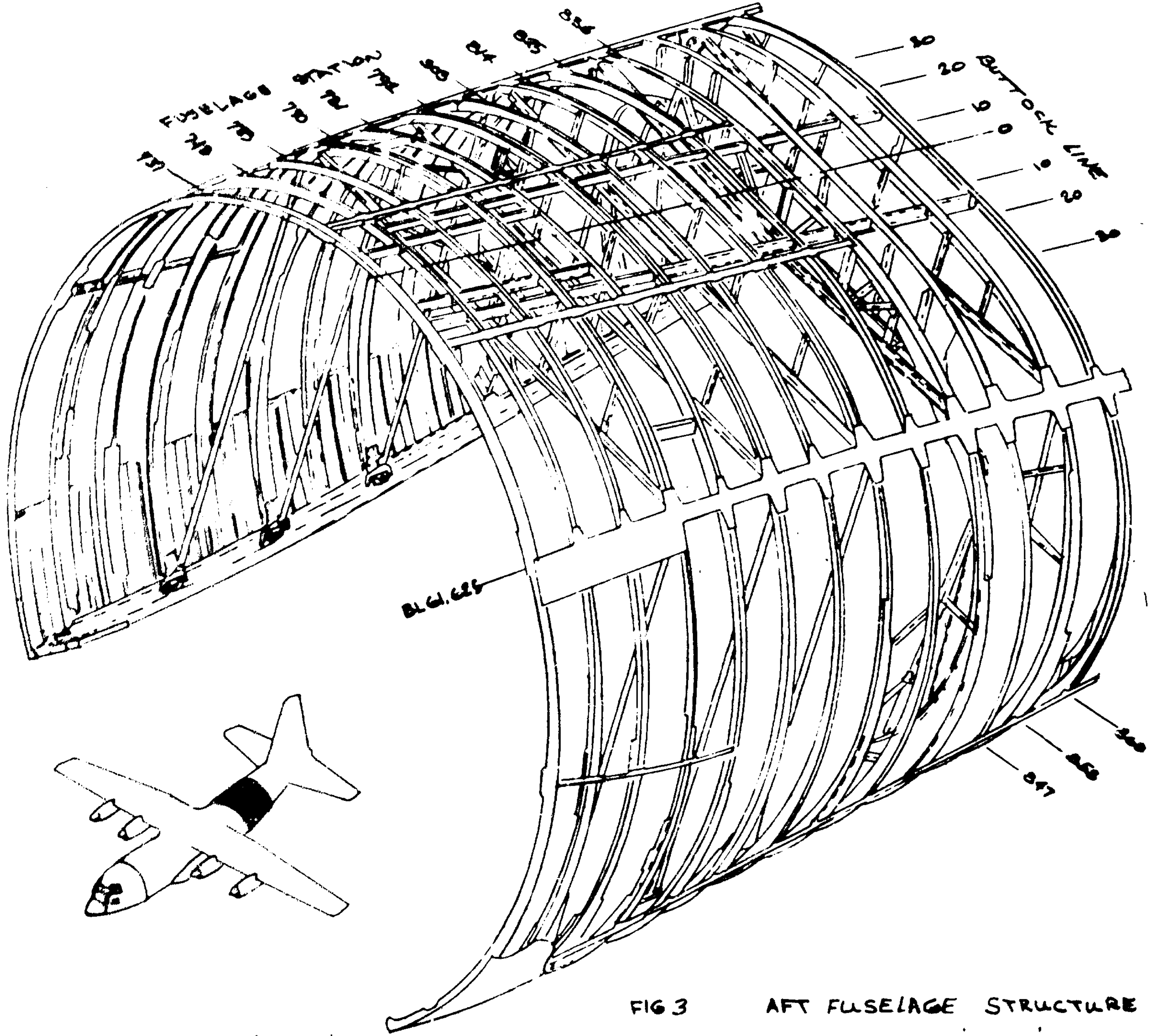

FIG 3 AFT FUSELAGE STRUCTURE

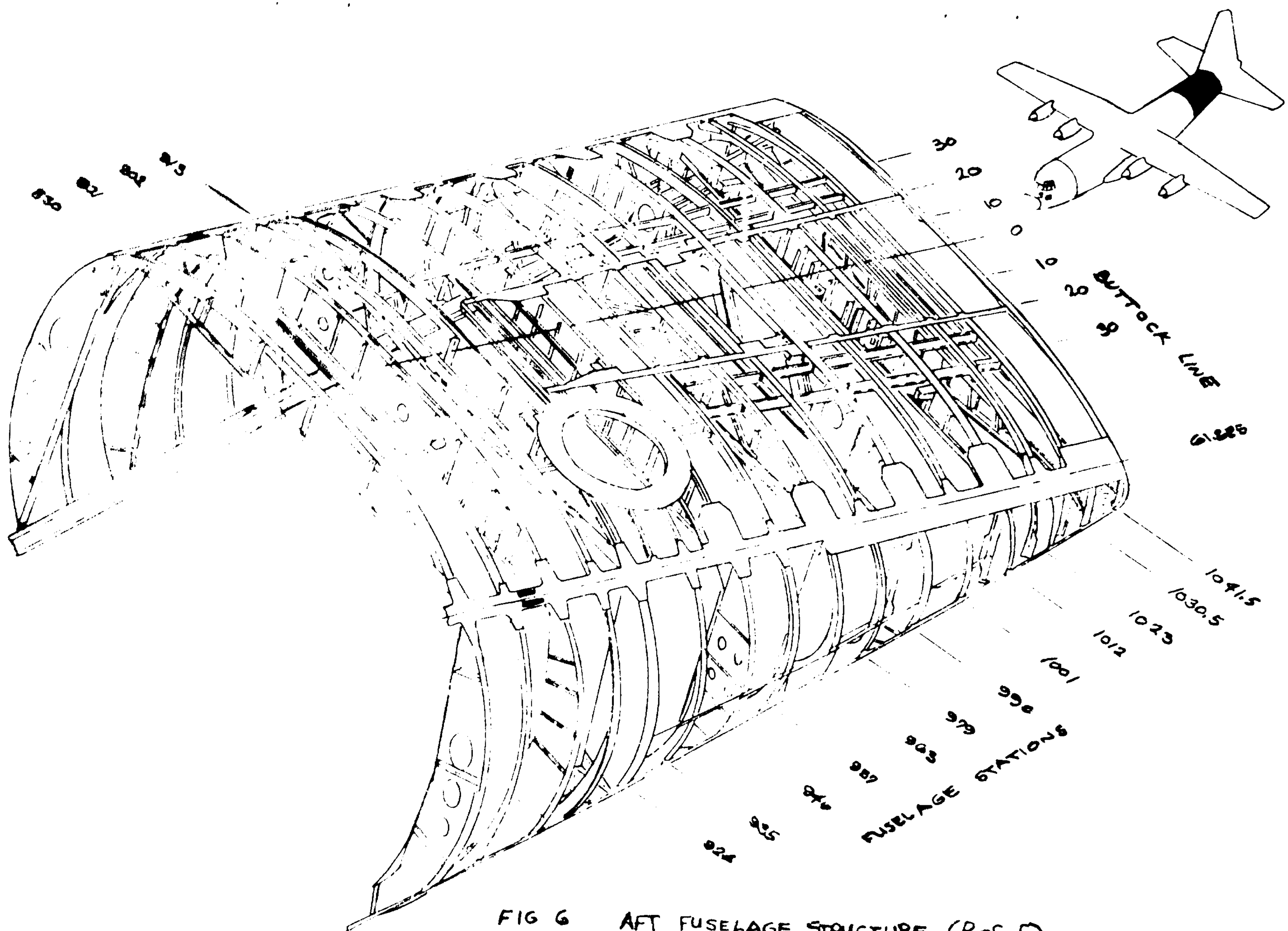

FIG 6 AFT FUSELAGE STRUCTURE (Ref. 5)

Gun mount gages (G). The two gages located on the 40mm gun mount are shown in Figure 7, below. Gage G1 measured the tipping load created by firing. This was accomplished by locating G1 on the elevation rod. Gage G2 was installed on the trunnion rod which is the primary member for transmitting the gun recoil into the mount.

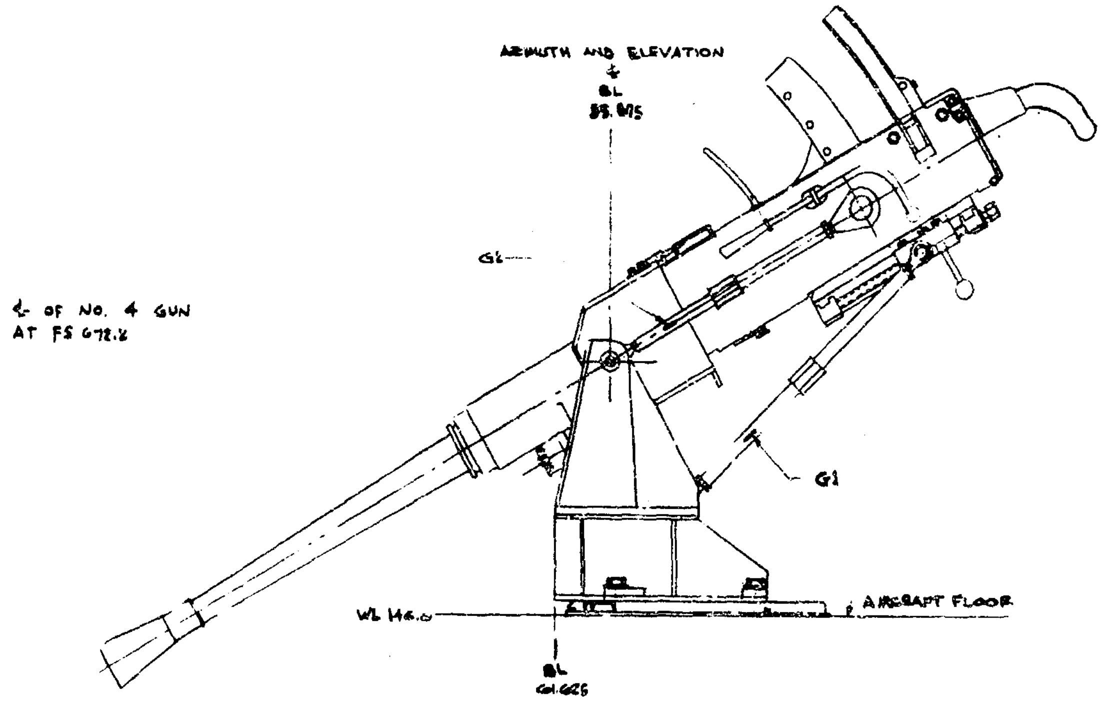

Figure 7 Number 4 40mm Gun

FLIGHT TEST

The flight test was conducted at Eglin AFB, Florida in September 1970 during simulated combat conditions in which other aircraft systems were being evaluated. The data was taken during test flights on 23, 24 and 30 September. The aircraft test bed was AC-130A, S/N 56-0490. Tests were conducted firing both 20mm Vulcan cannons and firing each 40mm Bofors individually. The pilot conducting the test had combat experience in AC-130A aircraft and closely simulated actual combat evasive maneuvers used in avoiding antiaircraft fire.

Pre-flight. Before each flight the DC offset of each amplifier was zeroed and all bridges were balanced using the bridge balance units. A milliammeter was used to balance each bridge. A signal was then recorded with the bridge balance units shorted out of the system to obtain the zero level of the amplifiers. Signals from each BBU were then recorded at the zero level.

In-flight. With the aircraft in straight and level flight, signals were recorded from each BBU to obtain the level flight strains. Data was then recorded using each BBU in turn while each 40mm gun was fired. Both single shot and rapid fire, bursts of two or more rounds at two rounds per second, were recorded. All data on the 20mm guns is for both guns firing simultaneously at a rate of 2450 rounds per minute for approximately one second. In addition, five antiaircraft evasive maneuvers were conducted, each one being recorded on a different BBU.

Post-flight. The tapes were played back and the signals transferred to oscillograph paper using a Honeywell Model 7600 Data Recorder at Flight Dynamics Laboratory, Wright-Patterson AFB, Ohio. Two passes were made at the data, one using no filter and one using a low pass filter with a cut off frequency of 280 hertz. The data was filtered to eliminate the 400 hertz signal supplied to the strain gages by the degraded power supply.

RESULTS

A summary of the test results is presented in Table III for the vertical stabilizer and in Table IV for the aft fuselage. Values presented are (1) stress changes due to level flight loads, $\Delta\sigma_{LF}$, (2) stress changes due to the left hand orbit, $\Delta\sigma_o$, (3) positive and negative over stresses produced by gun firing, $\Delta\sigma_+$ and $\Delta\sigma_-$. The positive and negative overstresses are then added (vectorially in the case of shear) to the mean stress level, $\Delta\sigma_o$, to yield the maximum and minimum stress changes, $\Delta\sigma_{max}$ and $\Delta\sigma_{min}$. The symbols are defined in Figure 23 (Appendix) for gun firings and for antiaircraft maneuvers.

Calculations. For all linear gages the stresses appearing in Table III and IV are normal stresses and in this case the maximum stress change, $\Delta\sigma_{max}$, is just the algebraic sum of the left hand orbit stress, $\Delta\sigma_o$, and the positive stress change due to gun firing, $\Delta\sigma_+$. But in the case of shear stresses, the strains had to be obtained from both the orbit traces and the gunfire traces. The differences between these two traces were not necessarily the same for all three gages in the rosette; therefore, the shear stresses for the left hand orbit maneuver and gun firing were obtained respectively from the left hand orbit strains and positive and negative gunfire strains separately. Then the sum of the strains due to both were added to yield the shear stress due to both the orbit and gun firing, using the standard equation for converting rosette strains to shear stresses. Hence, the sum of the shear stress due to the orbit and the shear stress due to gunfire does not equal the maximum shear stress. When reading Tables III and IV, care should be used in interpreting data from rosette gages, those using an R in their designation, for example VS18R. All stresses from rosette gages are in terms of shear stresses, since the design of all fuselage skin and beam webs was based on shear stress.

Level flight stresses. The stresses in Tables III and IV are presented in terms of changes in stress from the stress existing when the gages were installed. Observation of the level flight change in stress, Δ_{LF}, reveals that in the majority of cases stress levels remained constant from the installation condition to the level flight condition. Since positive loads are encountered on the horizontal stabilizer in flight and negative loads due to the dead weight are encountered in the installation condition, it is safe to conclude that the gages were installed at nearly a zero stress state.

Gun firing stresses. Sample traces are shown in Figures 24, 25, 26, 27, 28 and 29 for 40mm gun firings, in Figures 30 and 31 for 20mm gun firings and in Figure 32 for antiaircraft evasive maneuvers.

The highest normal stress recorded on the vertical stabilizer was 5128 psi compression on gage VS20 which is located on the rear beam fitting at VSS 0. This stress was produced when both 20mm guns were fired simultaneously. The highest shear stress recorded in the vertical stabilizer was 880 psi on gage VS4R, which was located on the rear beam shear web next to the lightening hold at VSS 10.88. This stress was recorded during the firing of Number 3 40mm gun.

Strains recorded on the two gages located on the 40mm gun were higher than those recorded during tests on the gun mount at Fort Carson, Colorado during August 1970. The probable cause of this was the more flexible platform, a sheet metal bed of a 2-1/2 ton truck used at Fort Carson. Subsequently more recoil was expended in truck deformation than occurs on the aircraft because of the more rigid mounting in the aircraft.

Evasive maneuver stresses. During an antiaircraft evasive maneuver a high normal stress in the aft fuselage of 3258 psi compression was recorded on gage AF6 which is located at the canted bulkhead at FS 847.

CONCLUSIONS AND RECOMMENDATIONS

The most obvious conclusion that can be made from a study of the data in Tables III and IV is that none of the loading mechanisms in question (i.e., 40mm gunfiring, 20mm gunfiring, or antiaircraft evasive maneuvers) impose loads on the aircraft approaching maximum design loads. All stresses measured were less than 10% of the design maximum stresses; they, therefore, present no foreseeable fatigue problems. In many cases the measured stresses were in the noise level of the recording system and are shown only for relative purposes.

Since the stress levels are quite low, it is difficult to form any definite conclusions as to the relative severity of stresses produced by 40mm gunfire versus 20mm gunfire. Overall results indicate that firing the 20mm guns simultaneously produced higher stresses on the majority of instrumented structure than did the 40mm gunfiring. This is understandable in that the 20mm guns have a much larger moment arm, from the aircraft center of gravity, than do the 40mm guns. Also when both 20mm guns are fired simultaneously, they produce roughly the equivalent recoil of one 40mm gun. Therefore, larger loads are produced in the vertical stabilizer to resist the moment produced by the 20mm gun firing than are produced when a single 40mm gun is fired. Although the 40mm guns are never fired simultaneously, both 20mm guns are fired simultaneously in the first burst, but subsequently are usually fired independently.

Since 40mm gunfiring introduces such small loads in the vertical stabilizer and aft fuselage, most of the recoil force is being expended in producing aircraft translational motion along the radius of the orbit (the aircraft is simply being pushed outward very slightly). Very little energy appears to be going into structural deformation. While the outward motion does not present a problem with the 40mm gun; it could present a more serious problem with a larger gun.

Multiple firings caused no amplification of stresses. The stresses measured for single firings were exactly the same as those measured for multiple firings (4-6 rounds fired at a rate of 2 rounds per second). It had been feared that the gunfiring grequency was quite near some of the fuselage's natural frequencies and might cause some dynamic magnification of stresses. This suspicion was found to be false.

If a larger gun is to be installed on an AC-130, the following instrumentation should be included, based on the results of the present test. Strain gages should be mainly concentrated in the immediate vicinity of the gun tiedown structure. A few gages should also be placed in the same positions as those in the report for comparison purposes.

LIST OF REFERENCES

1. Aft Fuselage Stress Analysis, Model C-130A. Lockheed Report No. ER 754M July 23, 1954.

2. Vertical Stabilizer Stress Analysis, Model C-130A. Lockheed Report No. ER 765M Jan 23, 1955.

3. Dally, J. W., and William F. Riley. Experimental Stress Analysis McGraw-Hill Book Company, Inc., New York, 1965.

4. Dave, Richard C., and Adams, P. H. Experimental Stress Analysis and Motion Measurement. 2nd Edition, Columbus, Ohio, Charles E. Merril Books, Inc., 1964.

5. AF Technical Order 1C-130A-3, Structural Repair.

APPENDIX

Preceding page blank

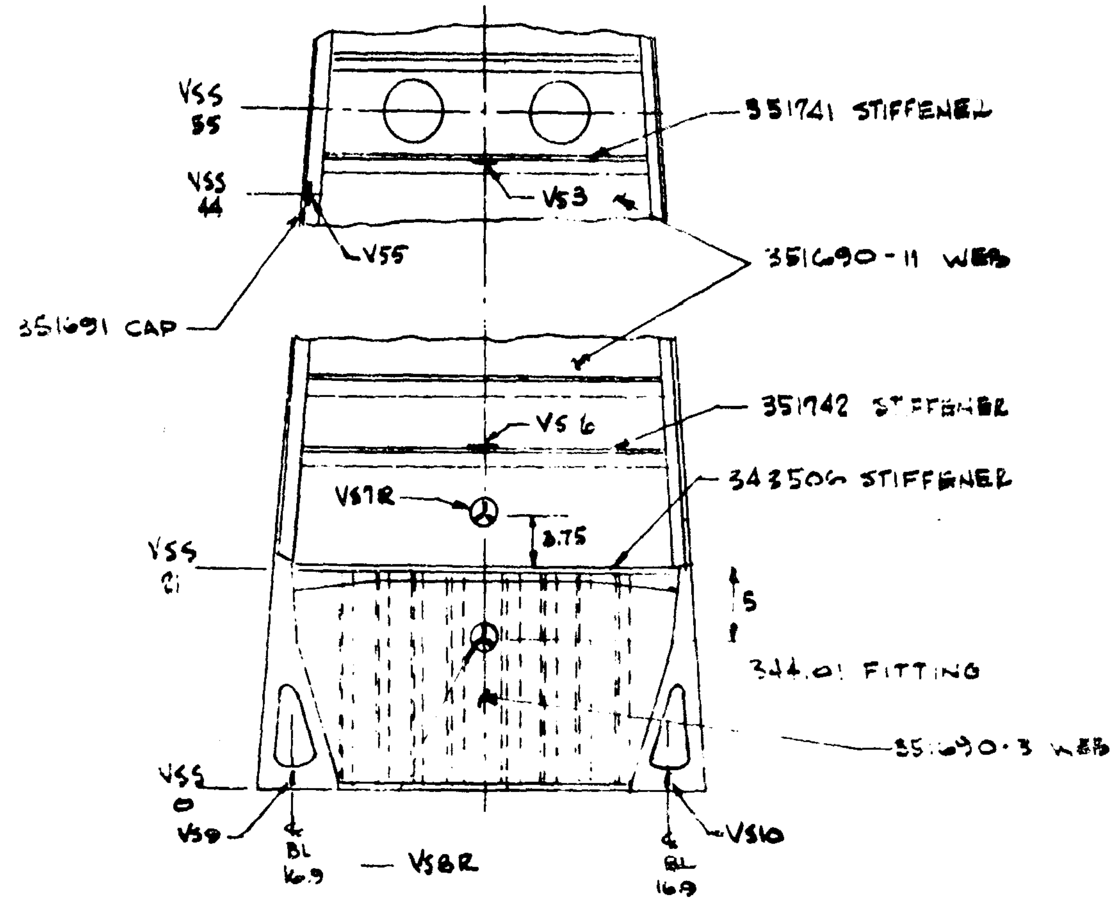

Fig. 8 VERTICAL STABILIZER - MAIN BEAM

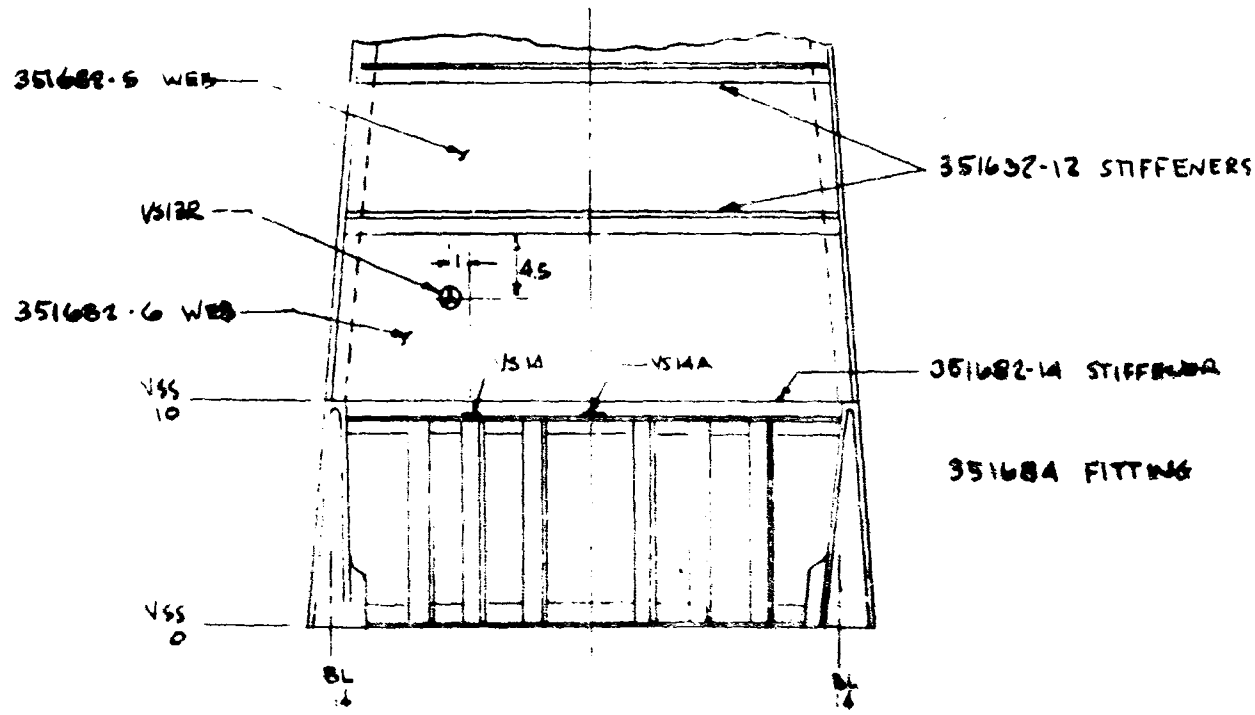

Fig 9. VERTICAL STABILIZER - AUXILIARY BEAM

Preceding page blank

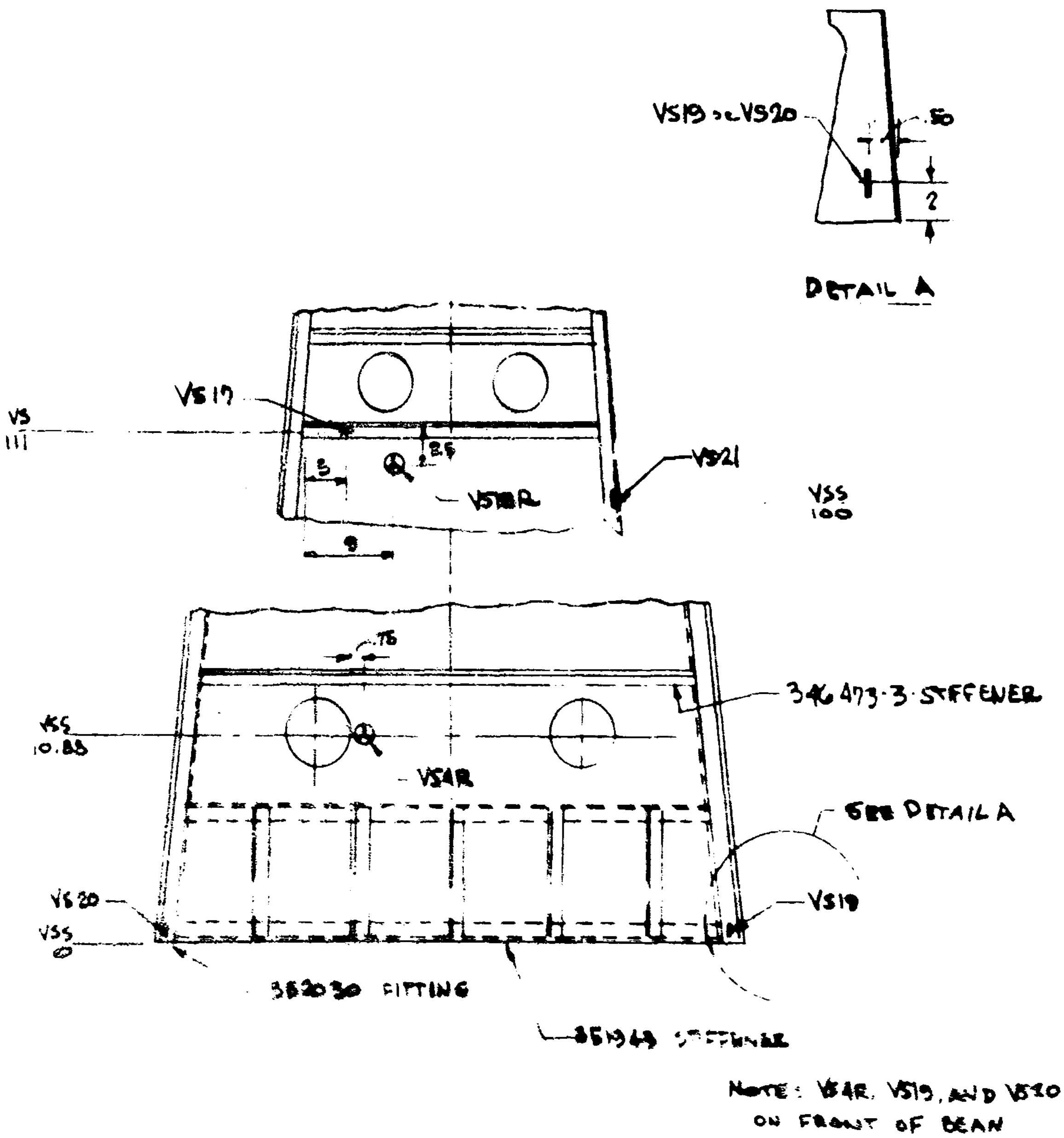

FIG 10 VERTICAL STABILIZER REAR BEAM
VIEW LOOKING FORWARD

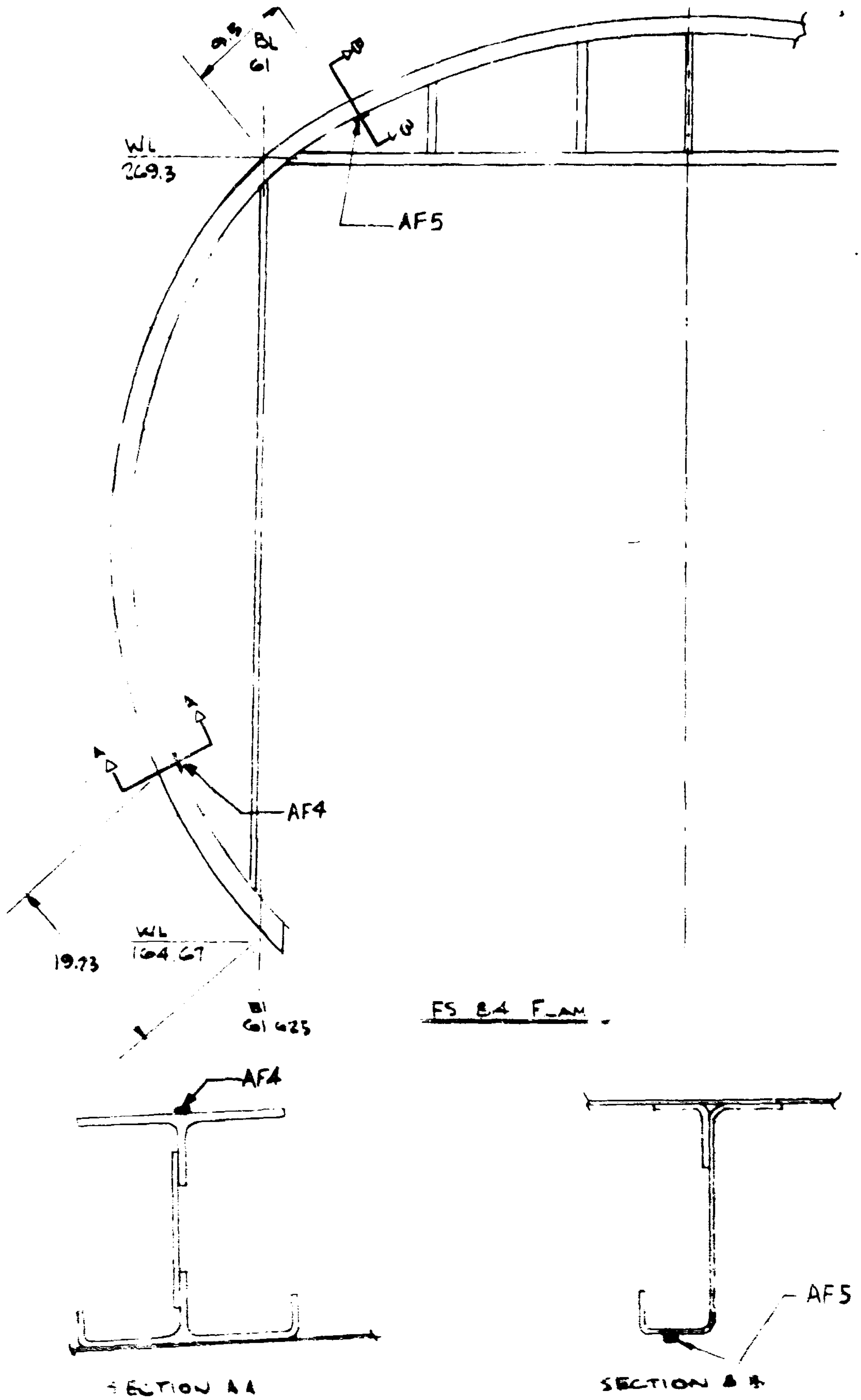

FIG 1: FS 84 FRAME

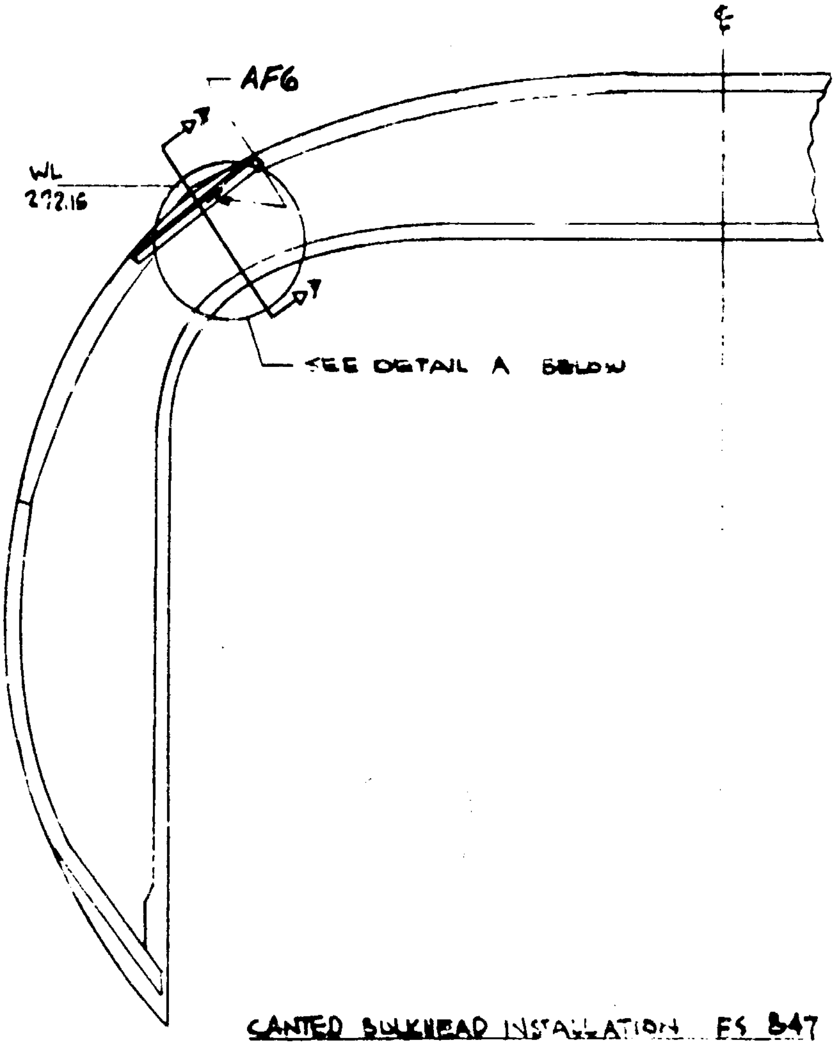

CANTED BULKHEAD INSTALLATION FS 847

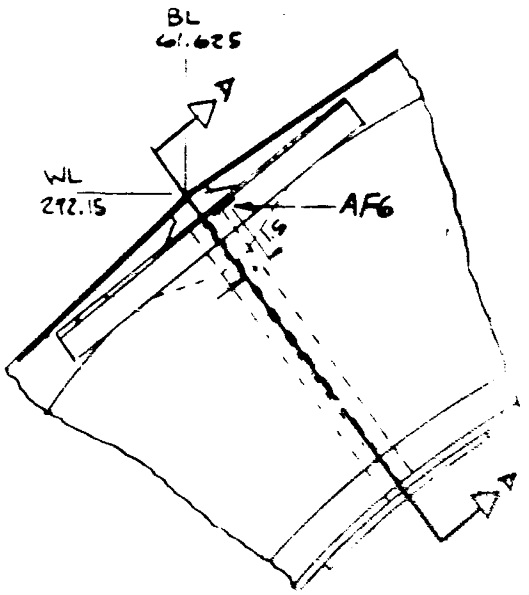

DETAIL A

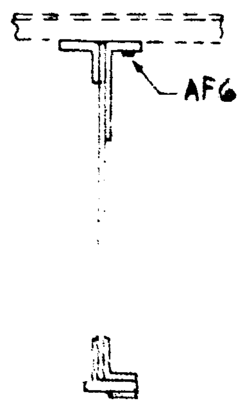

SECTION A-A

FIG 12 CANTED BULKHEAD INSTALLATION FS 847

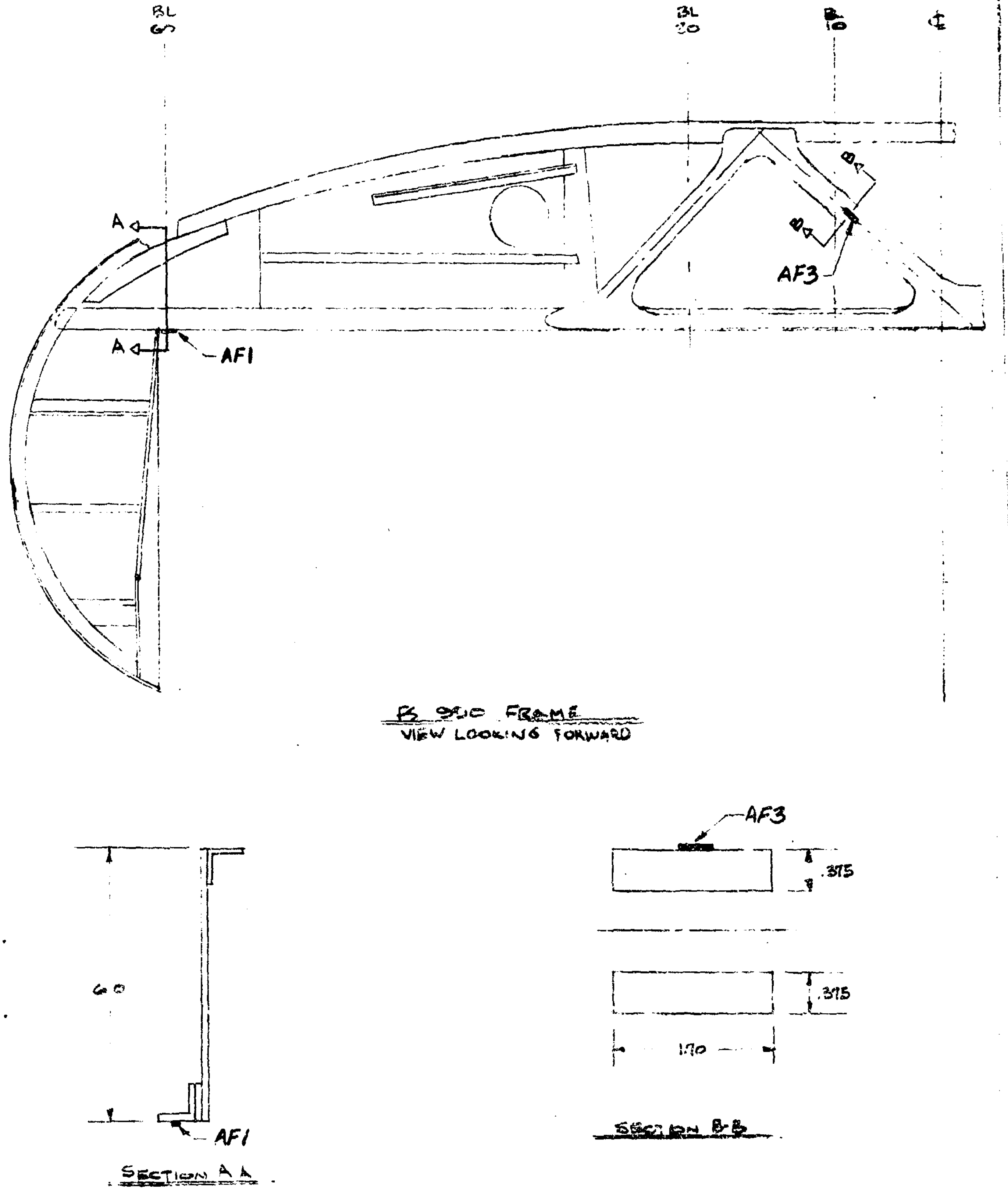

FIG 13 FS 990 FRAME

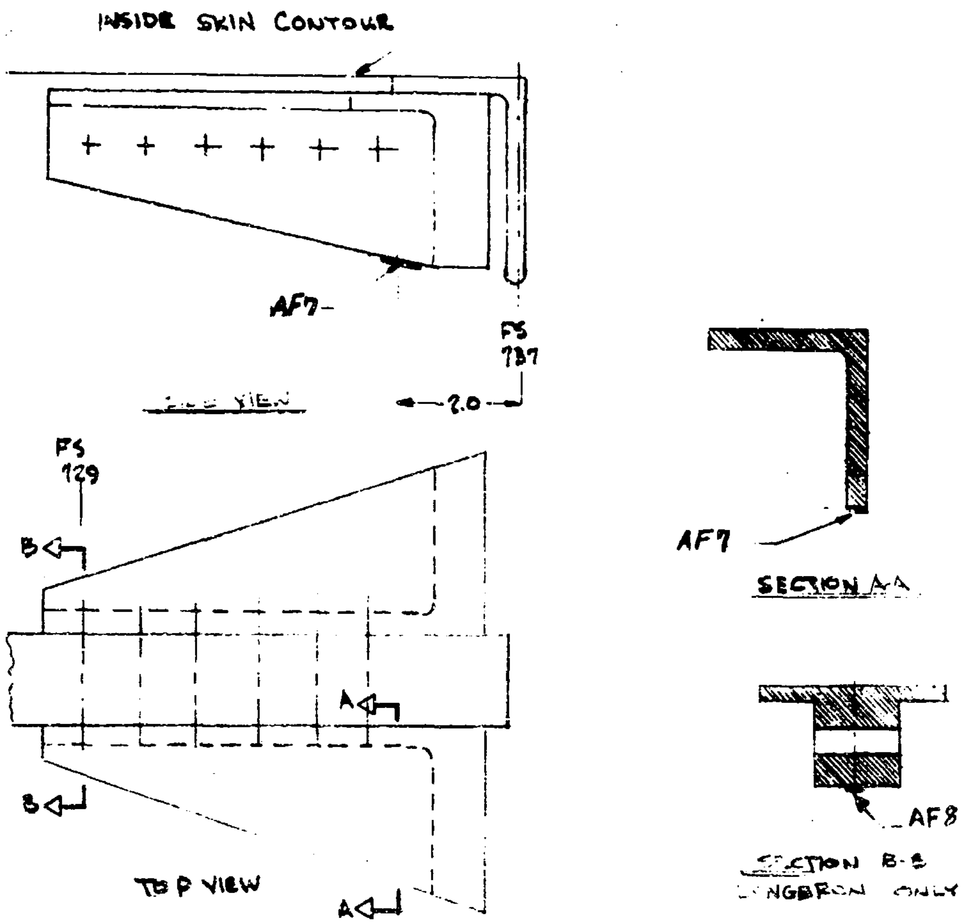

FIG 14 UPPER BL61 LONGERON FITTING F... AND LONGERON

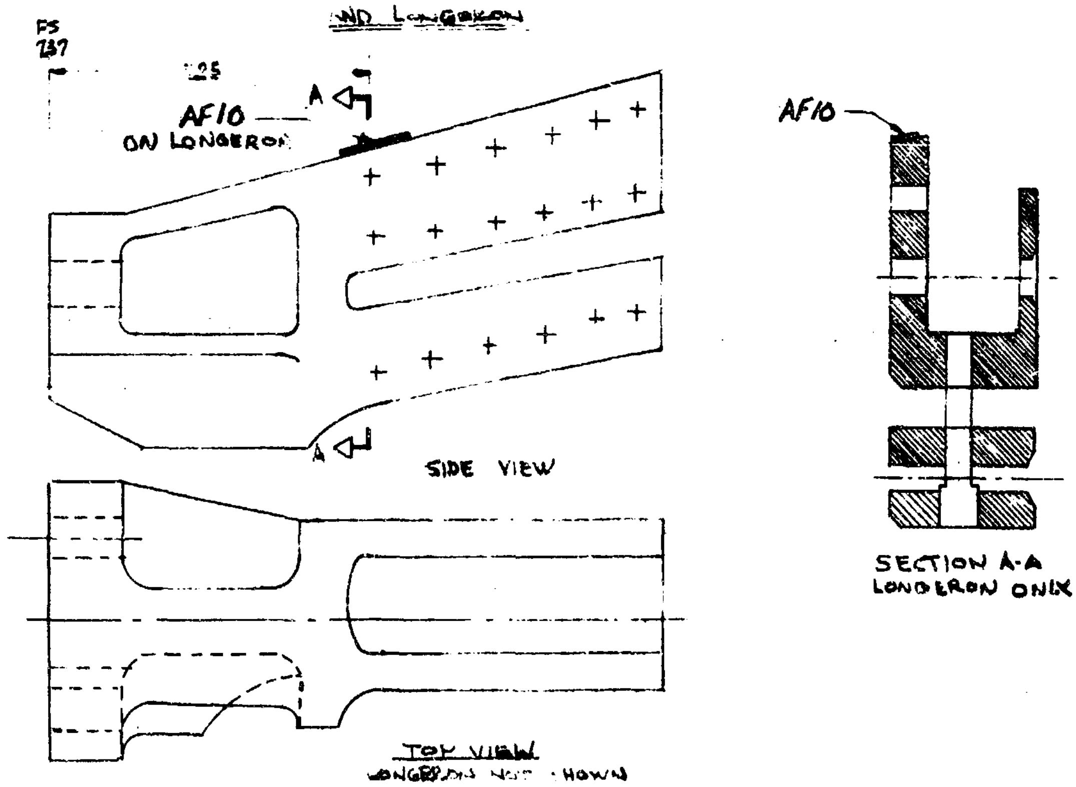

FIG 15 LOWER BL61 LONGERON FS 131 AFT

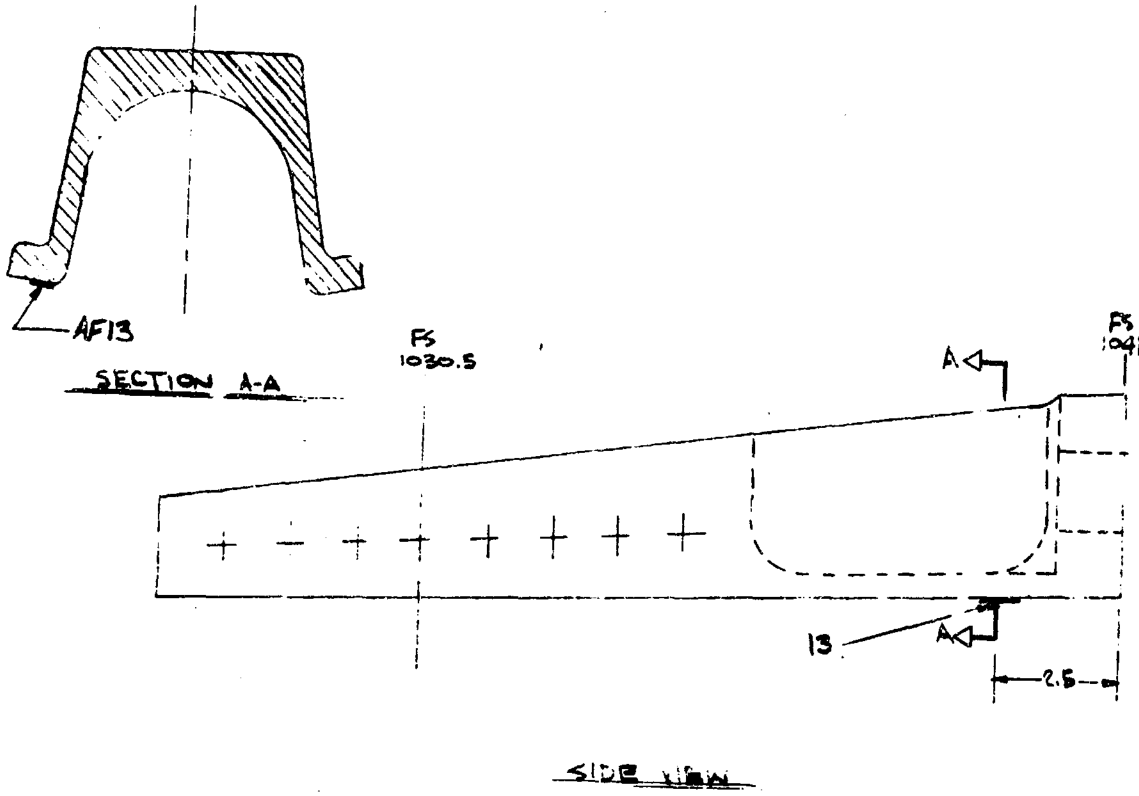

FIG 16 UPPER BL61 LONGERON FITTING FS 1041.5

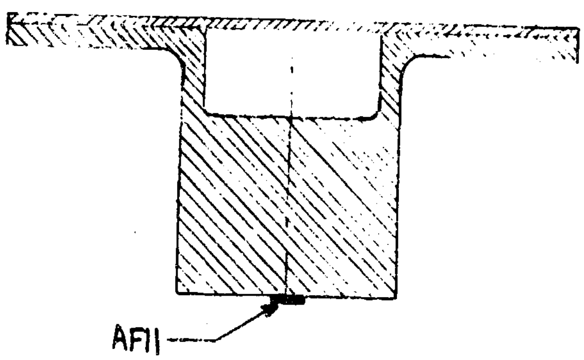

FIG 17 UPPER BL61 LONGERON SECTION AT FS 992

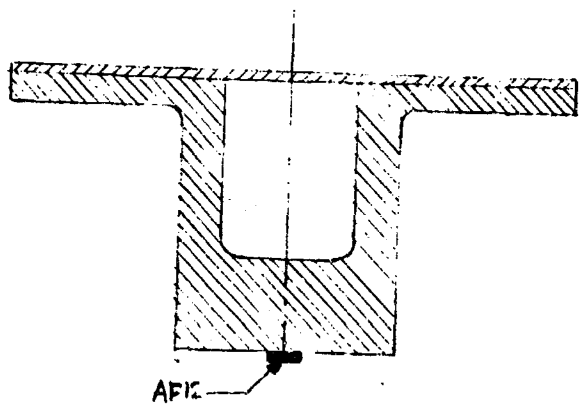

FIG 18 UPPER BL61 LONGERON SECTION AT FS 1020

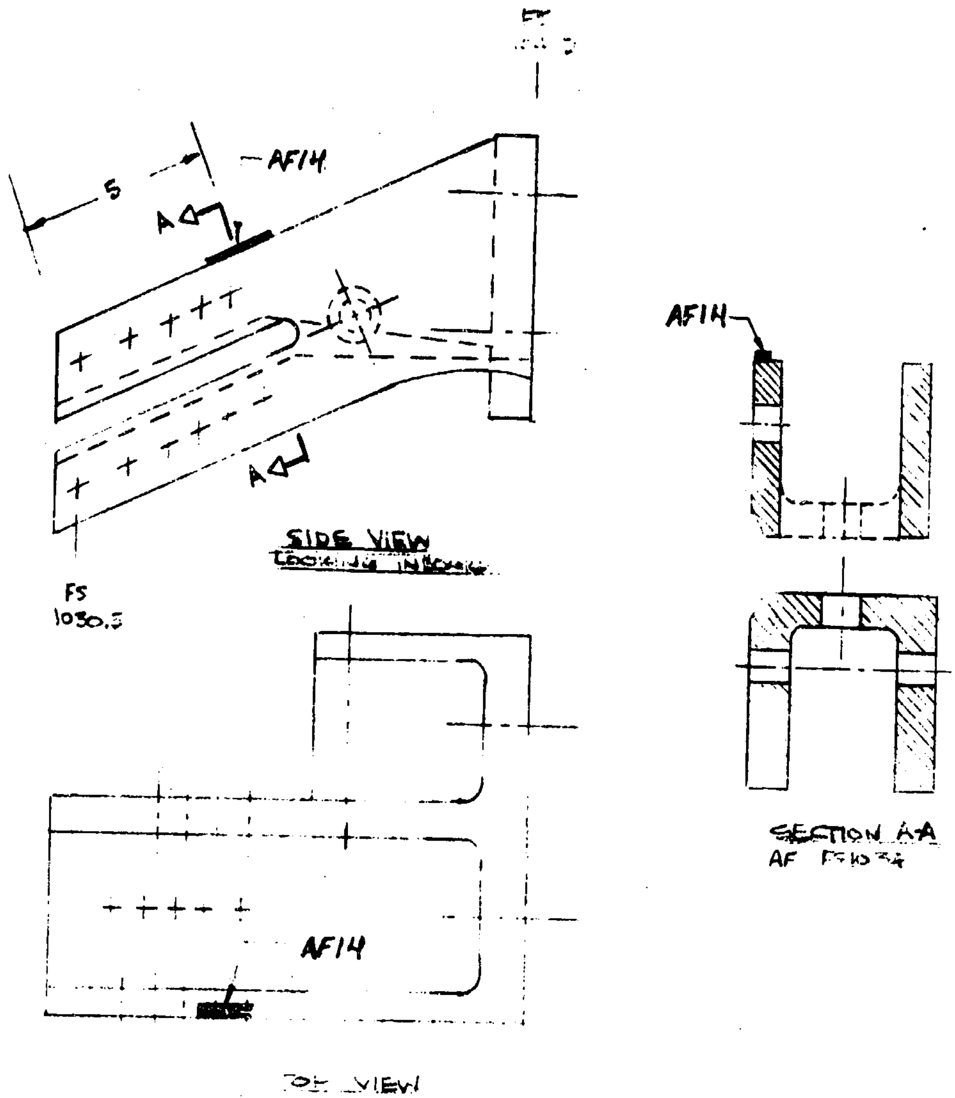

FIG 19 LOWER BL61 LONGERON FITTING FS 1041 FWD

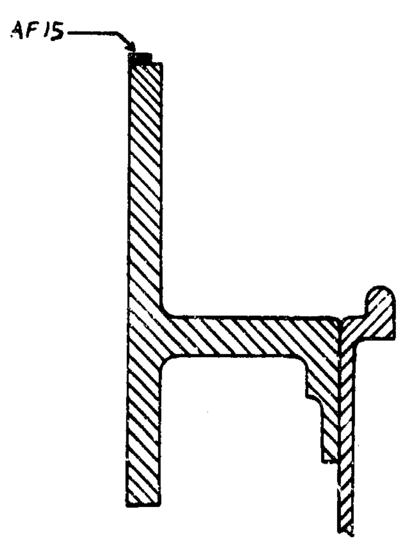

FIG. 20 Lower BL 61 Longeron Section At FS 1030

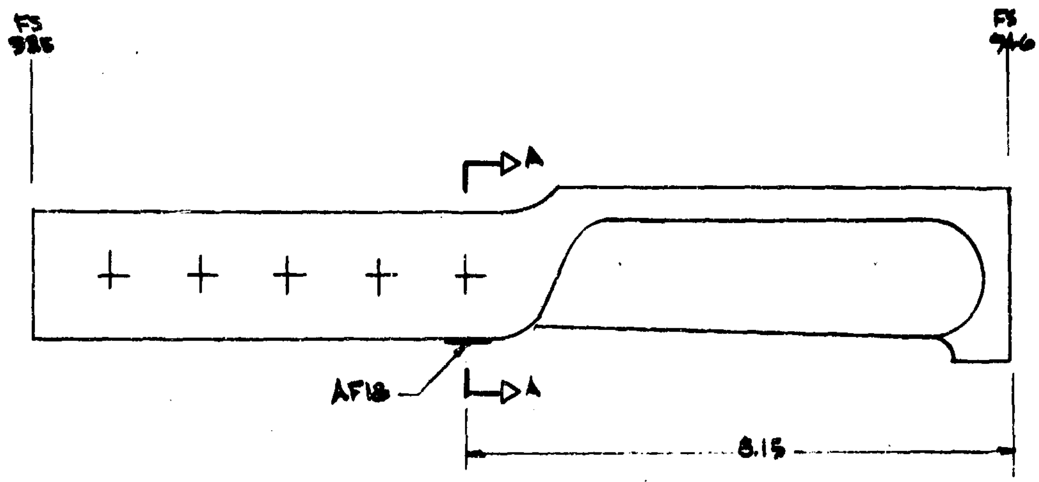

SIDE VIEW

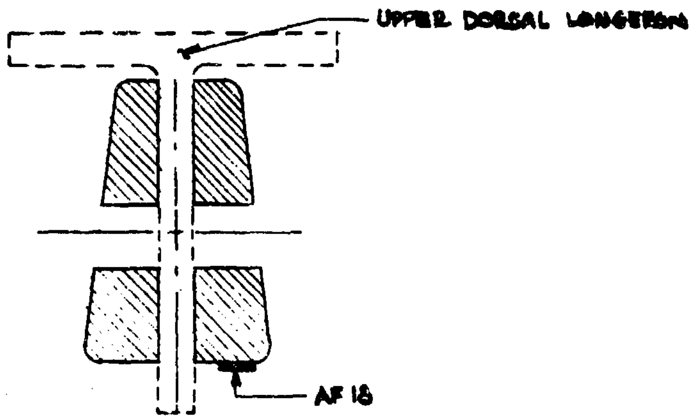

SECTION A-A

FIG 21 UPPER DORSAL LONGERON FITTING FS 946

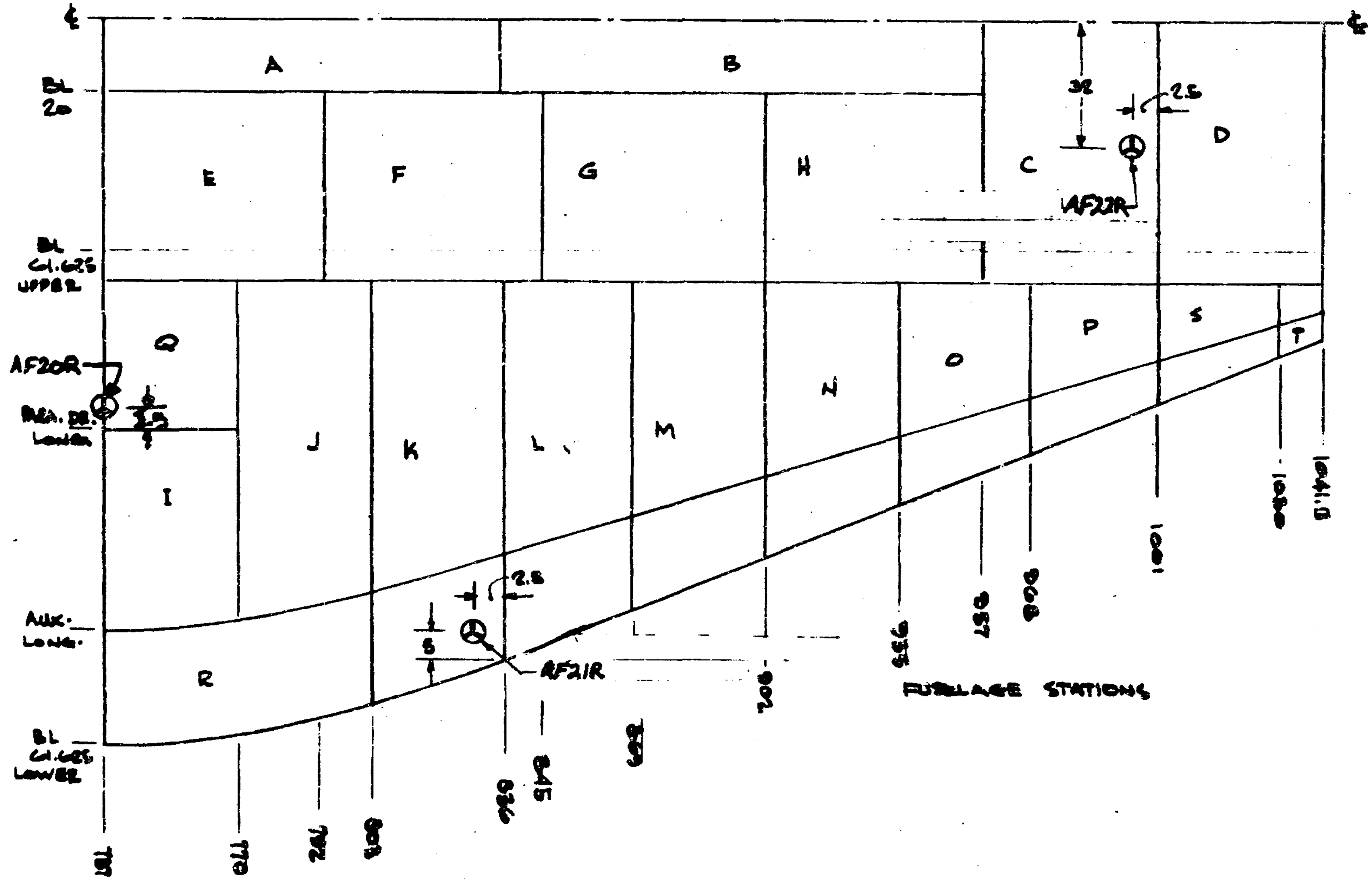

FIG 22 AFT FUSELAGE SKINS AND SPLICES

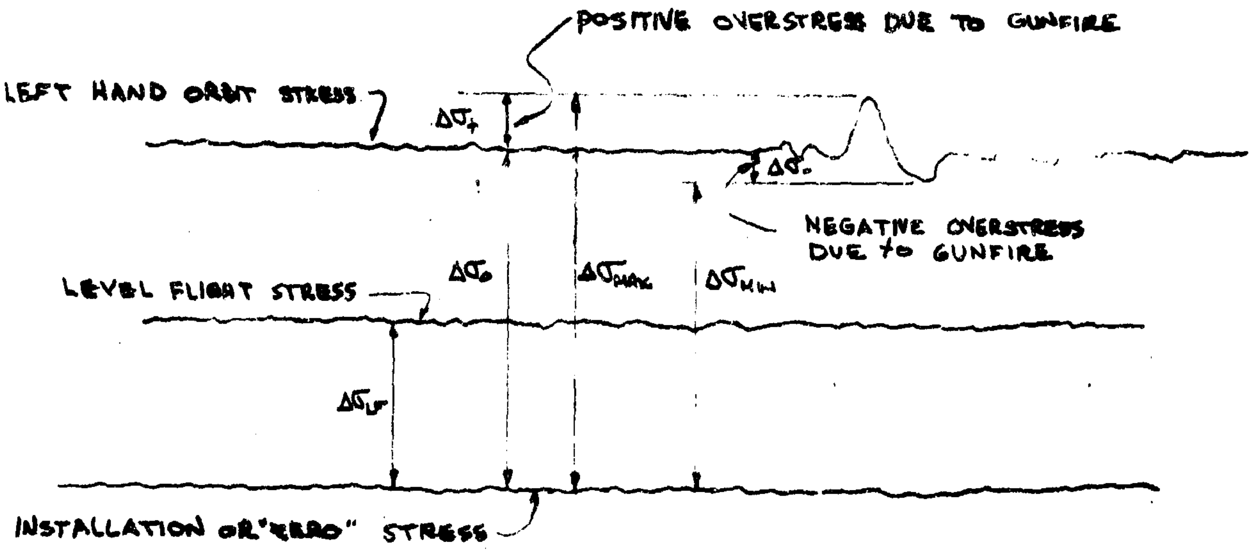

DEFINITION OF SYMBOLS FOR GUN FIRING STRESSES

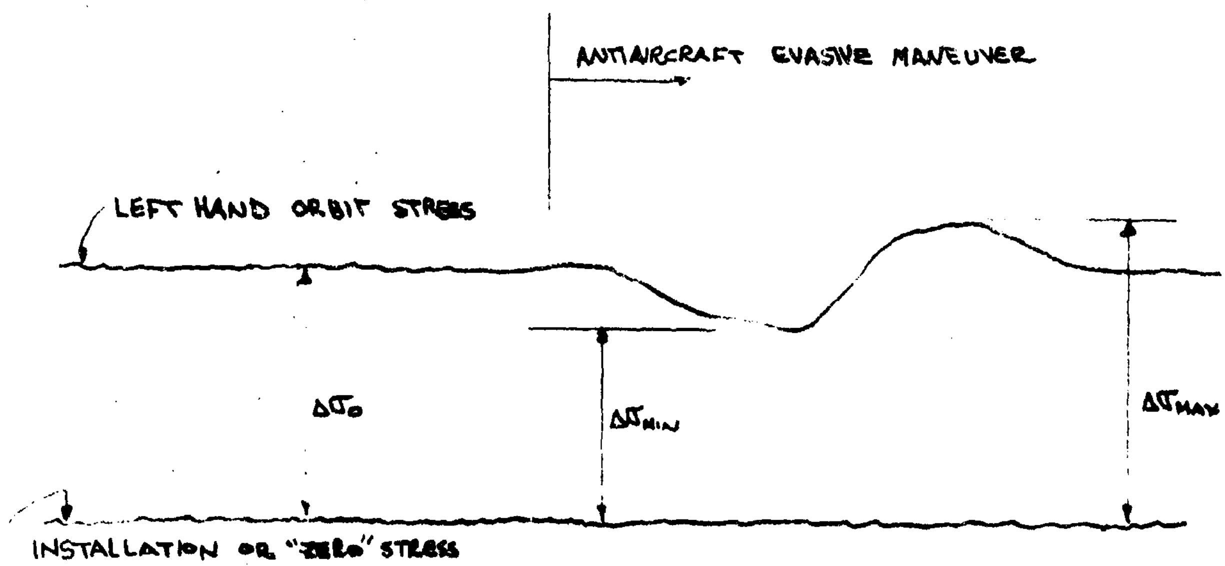

FIG 23 DEFINITION OF SYMBOLS IN TABLES III AND IV

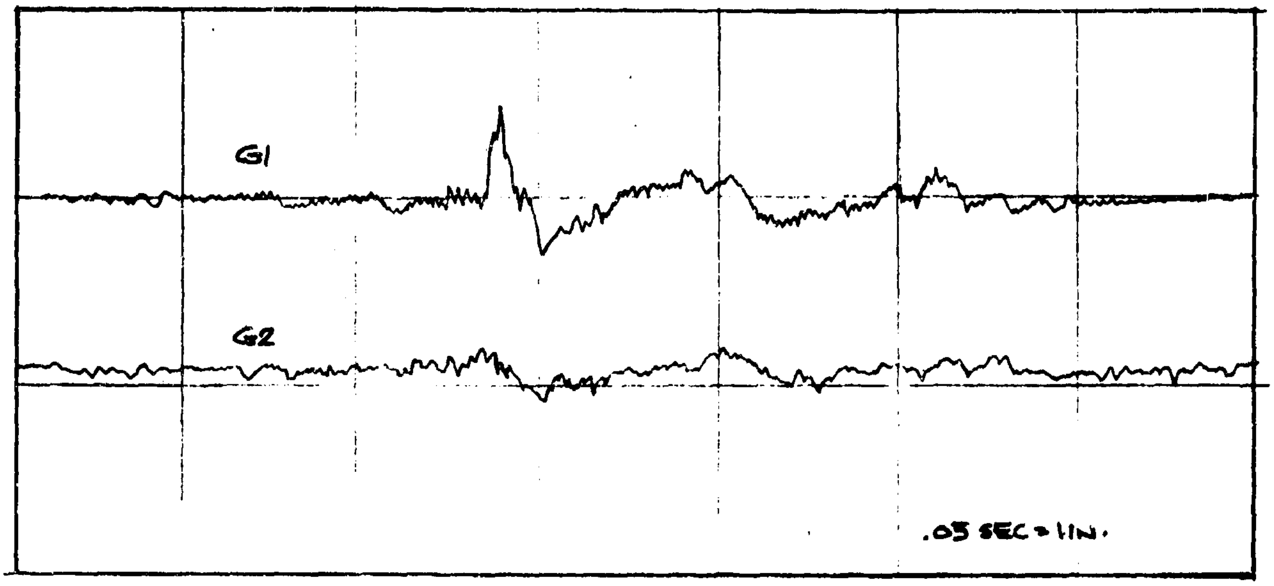

FIG 24 TYPICAL TRACE · 40 mm GAGES G1 AND G2

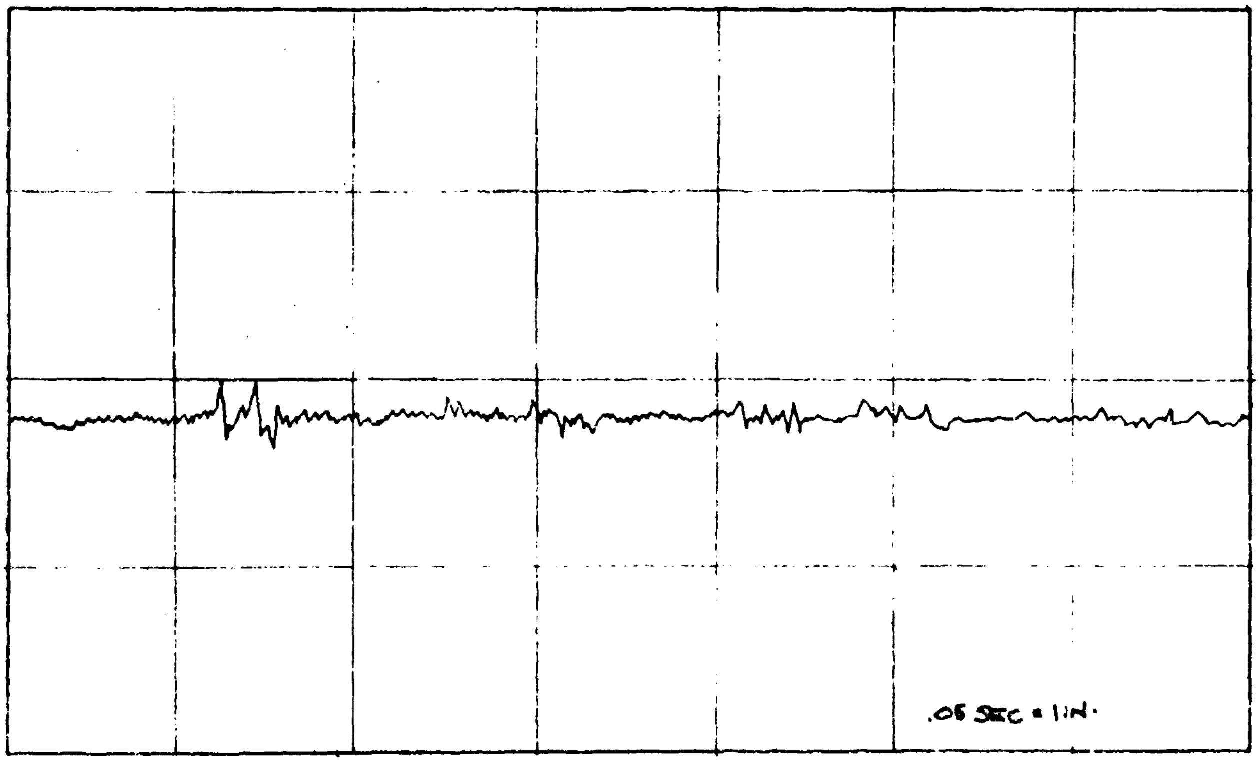

FIG. 25 TYPICAL TRACE · 40mm · GAGE AF13

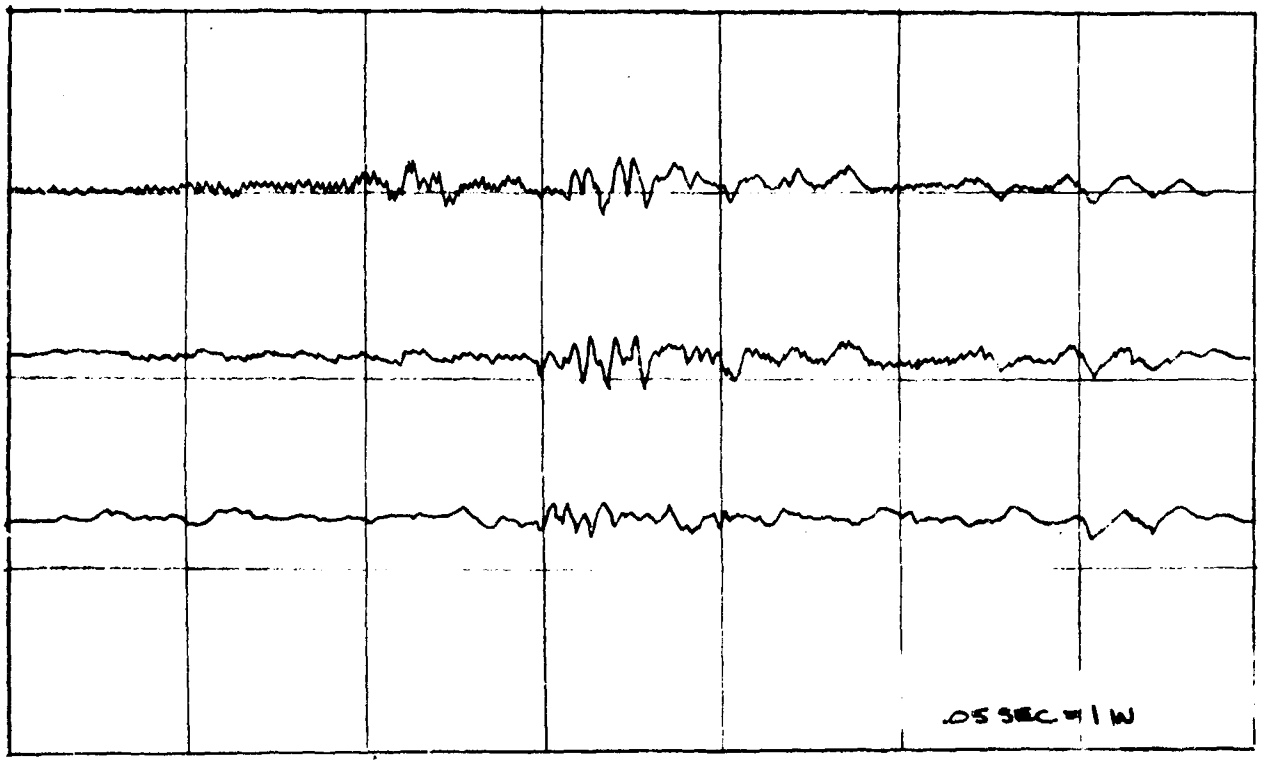

FIG 26 TYPICAL TRACE - 40mm - ROSETTE GAGE VS4R

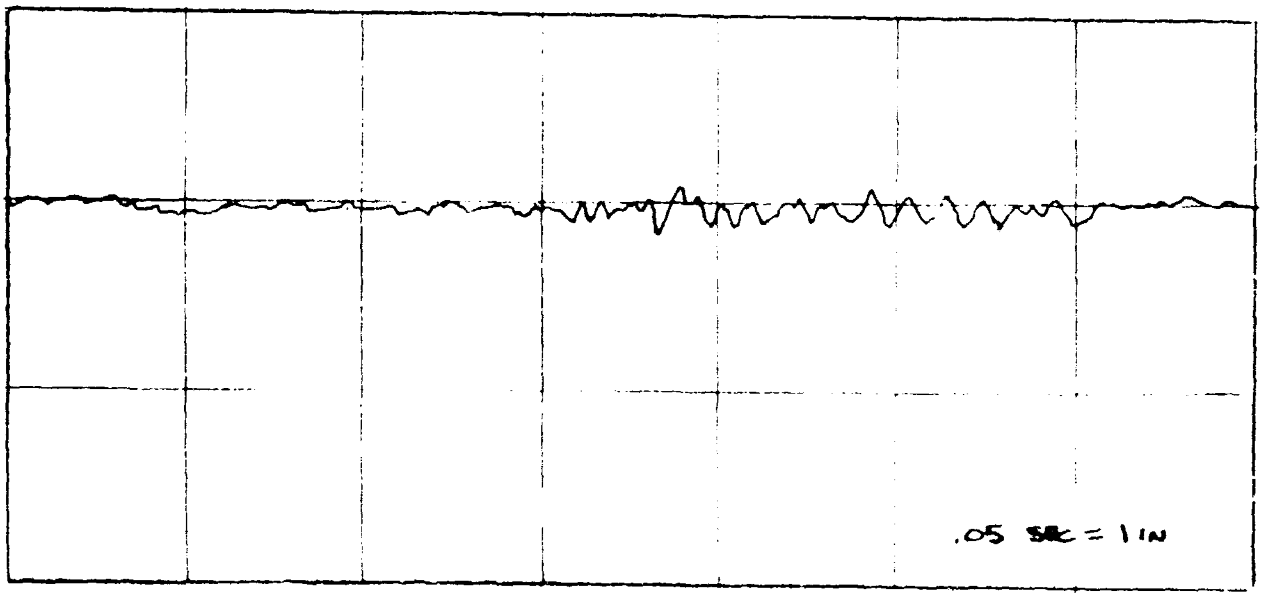

FIG 27 TYPICAL TRACE - 40mm - GAGE VSG

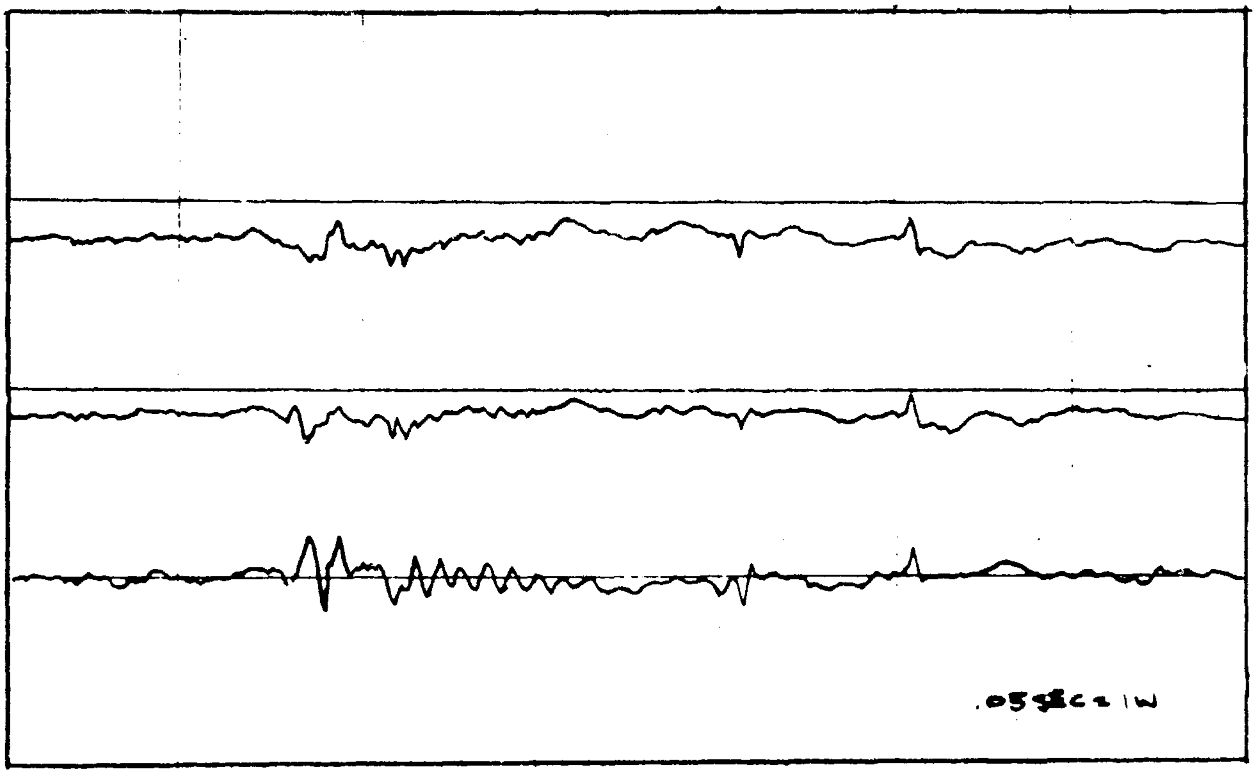

FIG. 28 TYPICAL TRACE . 40mm . ROSETTE GAGE AF21E

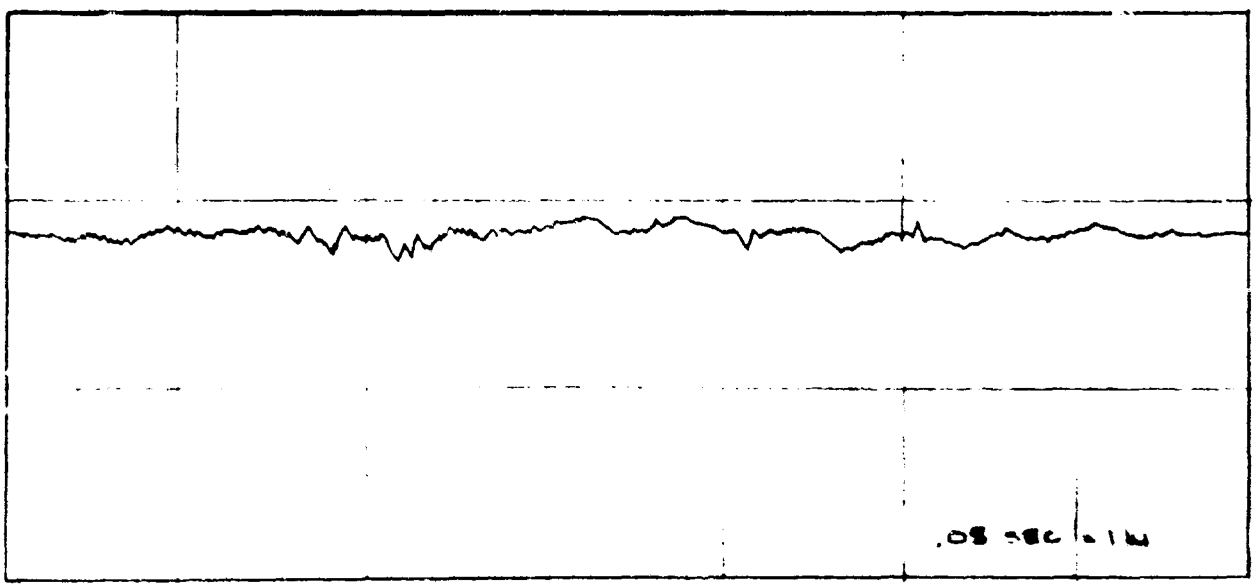

FIG. 29 TYPICAL TRACE . 40mm . GAGE AF10

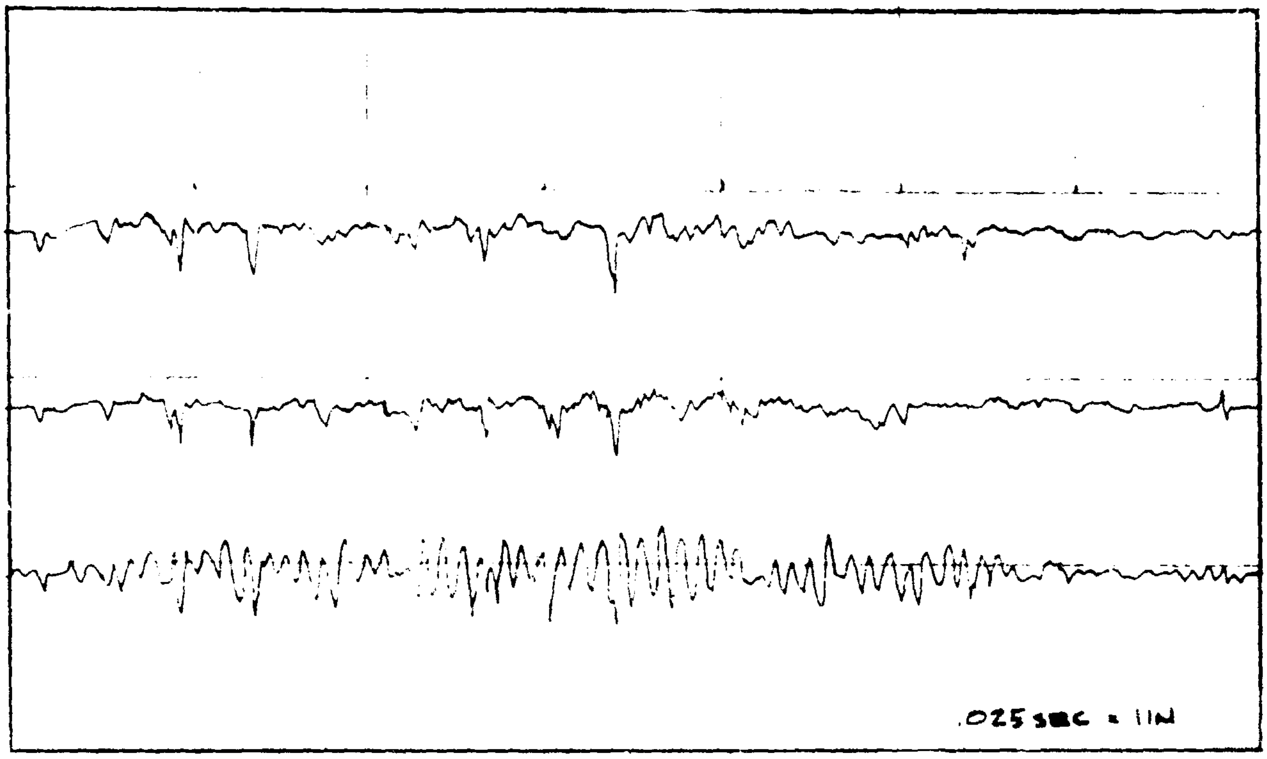

FIG. 30 TYPICAL TRACE 20mm ROSETTE GAGE AF21R

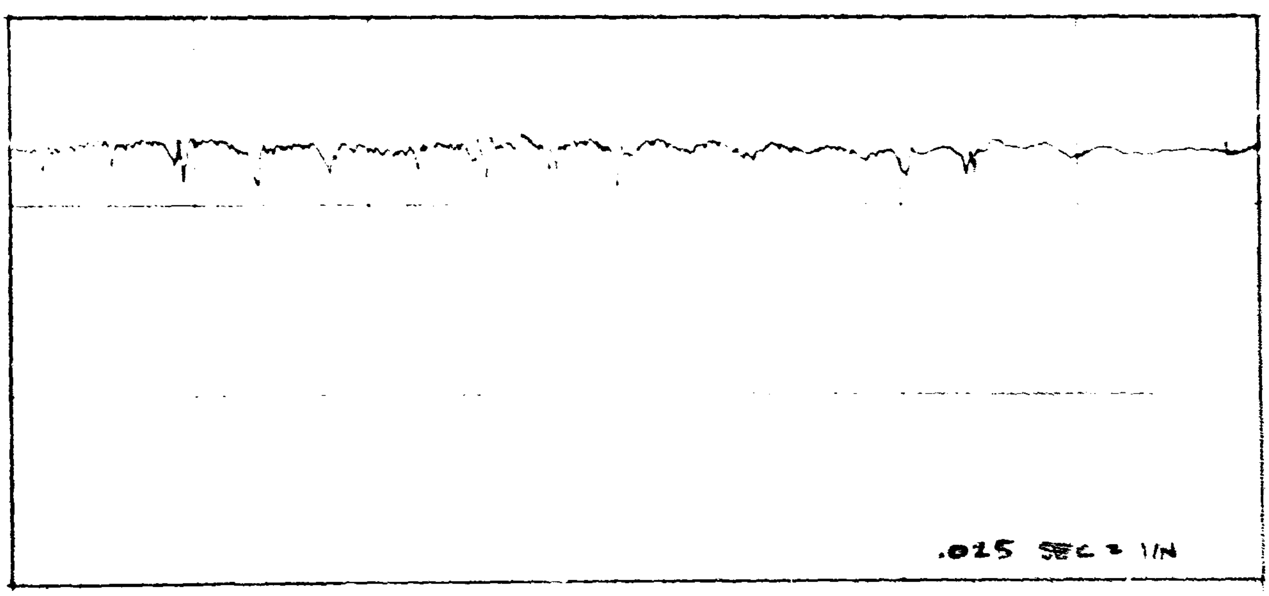

FIG 31 TYPICAL TRACE 20mm GAGE AF10

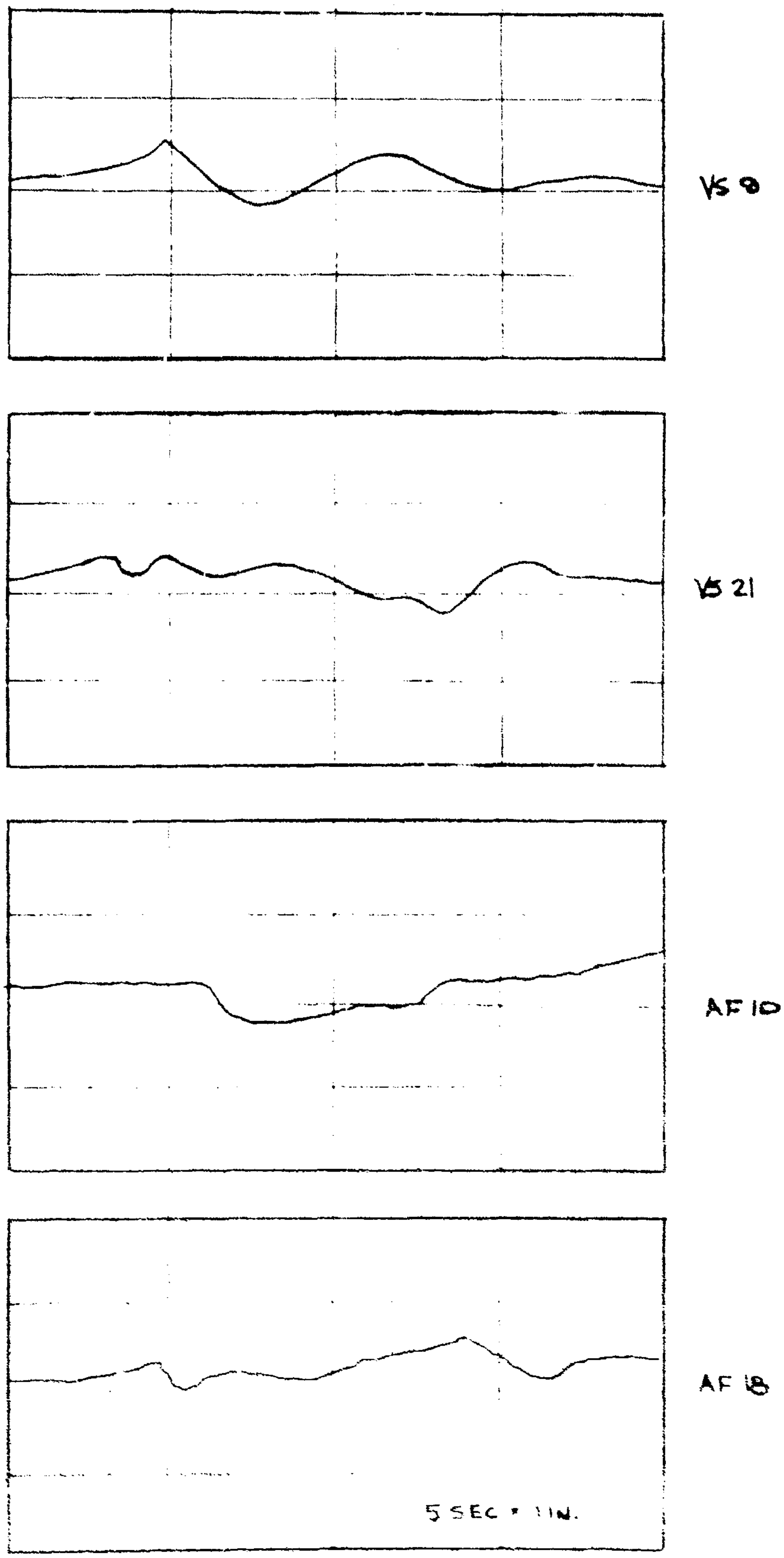

FIG 32 TYPICAL TRACES ANTIAIRCRAFT EVASIVE MANEUVERS

GAGE	FIGURE REF.	LOCATION	PART NO.	PART MAT'L.	CRITICAL DESIGN CONDITION	MINIMUM MARGIN OF SAFETY	DESIGN MODE OF FAILURE
VS3	3	Main Beam . Stiffener . VSS 45	351741	7075-T6 Extr.	A.P.C.[1]	0.08	Forced Crippling (B-48)
VS4R	5	Rear Beam . Shear Web . Next to Lightening Hole VSS 44	-	7075-T6 Clad	Zero[2] Yaw	-	Used Only As A Check On Shear Flow (B.50)[3]
VS5	3	Main Beam . Cap . VSS 44	351691	7075-T6 Extr.	A.P.C.	0.17	Crippling (B-49)
VS6	3	Main Beam . Stiffener . VSS 29	35172	2024-T4 Extr.	A.P.C.	0.00	Forced Crippling (B-45)
VS7R	3	Main Beam . Shear Web Panel at VSS 25	351690-11	7075-T6 Clad	A.P.C.	0.31	Web to Cap Attachment Bearing (B-46)
VS8R	3	Main Beam . Shear Web Panel at VSS 16	351690-3	7075-T6 Clad	A.P.C.	0.10	Web Attachment. Shear on DD6 Rivets, Brg 3/16" ST'L L'KB (B-43)
VS9	3	Main Beam . Fitting . VSS 0 B.L. 16.90	344101	2014-T6 Forg	A.P.C.	0.20	Attachment Main Beam Cap To Fitting. 1/4" Lock Bolts AWD
VS10	3	Main Beam . Fitting . VSS 0 B.L. - 16.90	344101	2014-T6 Forg	A.P.C.	0.20	NAS 336 . 3/8" Bolts in Shear and Bearing (B-70)
VS13R	4	Auxillary Beam Shear Web Above VS 10 Stiffener	351682-6	2024-T4 Clad	A.P.C.	-	Used Only As Check On Shear Flow (g=183 lb/in) (B-36)
VS14	4	Auxillary Beam. Stiffener. VSS 10	351682-14	7075-T6 Extr.	A.P.C.	0.23	End Connection - 2-1/4" St'l LKB & 2-DD6 Rivets - BRG (B-36)

Table I, Page 1

SUMMARY OF VERTICAL STABILIZER STRAIN GAGE LOCATIONS

GAGE	FIGURE REF.	LOCATION	PART NO.	PART MAT'L.	CRITICAL DESIGN CONDITION	MINIMUM MARGIN OF SAFETY	DESIGN MODE OF FAILURE
VS14A	4	Duplicate of VS14	351682-14	7075-T6 Extr.	A.P.C.	0.23	End Connection - 2-1/4" ST'L LKB 2-DD6 Rivets - BRG (B-36)
VS17	5	Rear Beam - Stiffener VSS 111	-	7075-T6 Extr.	Zero Yaw	-	Used Only As A Check On Axial Load Since Critical Stiffener at VSS 120 was Inaccessible.
VS18R	5	Rear Beam - Shear Web Panel Between VSS 92 and VSS 111	-	7075-T6 Clad	Zero Yaw	-	Used Only As A Check On Shear Flow Since Critical Panel at VSS 127 - VSS 142 was Inaccessible.
VS19	5	Rear Beam - Fitting - VSS 0	352030	8630 ST'L	A.P.C.	0.01	Bending (B-71)
VS20	5	Rear Beam - Fitting - VSS 0	352030	8630 ST'L	A.P.C.	0.01	Bending (B-61)
VS21	5	Rear Beam - Cap at VSS 100	351703	7075-T6 Extr.	A.P.C.	0.27	Crippling (B-55)

1. Asymmetric Power Condition
2. Instantaneous Rudder
3. Refers to Theoretical Stress Analysis See Ref. 1.

Table I, Page 2

GAGE	FIGURE REF.	LOCATION	PART NO.	PART MAT'L.	CRITICAL DESIGN CONDITION	MINIMUM MARGIN OF SAFETY	DESIGN MODE OF FAILURE
AF1	6	FS 990 Frame. Bottom. Section A-A		7075-T6 Extr.	A.P.C.	0.01	Tension (A-82)[2]
AF3	6	FS 990 Frame. Middle. Section B-B		7075-T6 Extr.	A.P.C.	0.20	Compression (A-85)
AF4	7	FS 814 Frame. Outside. Section A-A		7075-T6 Extr.	A.P.C.	0.01	Compression (264)
AF5	7	FS 814 Frame. Top. Section B-b		7075-T6 Extr.	15 psi	0.18	Compression (264)
AF6	8	FS 847. Canted Blk Hd. Section A-A		7075-T6 Extr.	Cargo Log.	0.08	Tension (269)
AF7	9	Upper BL 61 Fitting FS 735 FWD.		7075-T6 Extr.	MANV.	0.07	Tens. + Bending (188)
AF8	10	Upper BL 61 Longeron FS 729 Section Through Bolt 1	337929	7075-T6 Extr.	MANV.	0.00	Tens. + Bending (189)
AF10	11	Lower BL 61 Fitting FS 744 AFT Section C-C		7075-T6 Forg	LAT.GUST	0.06	Comp. + Bending (169)
AF11	12	Upper BL 61 Longeron FS 992		7075-T6 Extr.	LAT.GUST	0.03	Compression (195)
AF12	13	Upper BL 61 Longeron FS 1020		7075-T6 Extr.	LAT.GUST	0.17	Compression (193)
AF13	14	Upper BL 61 Fitting FS 1039 Sec B-B	337595	7075-T6 Forg	LAT.GUST	0.12	Tens. + Bending (194)

Table II, Page 1

SUMMARY OF AFT FUSELAGE AND GUN STRAIN GAGE LOCATIONS

GAGE	REF.	LOCATION	PART NO.	PART MAT'L	CRITICAL DESIGN CONDITION	MINIMUM MARGIN OF SAFETY	DESIGN MODE OF FAILURE
AF14	15	Lower BL 61 Fitting FS 1034 Sec A-A	337426	7075-T6 Forg	LAT.GUST	0.04	Comp. + Bending (176)
AF15	16	Lower BL 61 Longeron FS 1030		7075-T6 Extr.	LAT.GUST	0.00	Comp. + Bending (176)
AF18	17	Fitting Upper Dorsal Longeron FS 946 Section C-C		7075-T6 Forg	MANV.	0.02	Tens + Bending (133)
AF20R	18	Fuselage Skin FS 741 Upper BL 79 Panel Q		7075-T6 CLAD	A.P.C.	0.05	Shear (A-75)
AF21R	18	Fuselage Skin FS 833 Lower BL 54 Panel K		7075-T6 CLAD	A.P.C.	0.07	Shear (A-71)
AF22R	18	Fuselage Skin FS 1000 Upper BL 32 Panel C		7075-T6 CLAD	A.P.C.	0.48	Shear (A-64)
G1	19	40mm Gun. Elevation Rod		Steel	Recoil	Large	Compression
G2	19	40mm Gun. Trunnion Rod		Steel	Recoil	Large	Tension

1. Asymmetric Power Condition
2. Refers to Theoretical Stress Analysis, See Ref 2.

Table II, Page 2

GAGE	FIGURE REF.	LOCATION	$\Delta\sigma_{LF}$*	$\Delta\sigma_o$	CONDITION	$\Delta\sigma_+$	$\Delta\sigma_-$	$\Delta\sigma_{max}$	$\Delta\sigma_{min}$
VS3	3	Main Beam Stiffener at VSS 45	0	0	40mm	169	-474	169	-474
					20mm	507	-846	507	-846
					AAA	-	-	0	0
VS4R	5	Rear Beam Shear Web Next to Lightening Hole at VSS 10.88	319	727	40mm	347	236	839	676
					20mm	132	109	600	617
					AAA	-	-	727	629
VS5	3	Main Beam Cap at VSS 44	0	-285	40mm	357	-357	71	-642
					20mm	428	-607	143	-892=
					AAA	-	-	250	-750
VS6	3	Main Beam Stiffener at VSS 29	0	183	40mm	367	-550	550	-183
					20mm	183	-734	3678	-550
					AAA	-	-	550	183
VS7R	3	Main Beam Shear Web Panel at VSS 25	0	190	40mm	158	262	210	239
					20mm	119	86	253	224
					AAA	-	-	327	192
VS8R	3	Main Beam Shear Web Panel at VSS 16	0	277	40mm	100	181	316	183
					20mm	50	229	227	102
					AAA	-	-	77	138
VS9	3	Main Beam Fitting at VSS 0, BL +16.9	0	0	40mm	338	-609	338	-609
					20mm	677	-677	677	-677
					AAA	-	-	846	-338
VS10	3	Main Beam Fitting at VSS 0, BL -16.9	0	0	40mm	673	-798	678	-798
					20mm	399	-598	399	-598
					AAA	-	--	997	-399
VS13R	4	Auxillary Beam Shear Web Above VSS 10 Stiffener	152	394	40mm	50	77	363	442
					20mm	201	219	645	176
					AAA	--	-	45	-88

Table III, Page 1

EXPERIMENTAL STRESS VERTICAL STABILIZER

GAGE	FIGURE REF.	LOCATION	$\Delta\sigma_{LF}$*	$\Delta\sigma_o$	LOCATION	$\Delta\sigma_+$	$\Delta\sigma_-$	$\Delta\sigma_{max}$	$\Delta\sigma_{min}$
VS14	4	Auxillary Beam Stiffener at VSS 10	0	367	40mm	293	-403	660	-37
					20mm	293	-734	660	-367
					AAA	-	-	367	367
VS17	5	Rear Beam Stiffener at VSS 111	0	74	40mm	444	-444	518	-370
					20mm	370	-666	444	-592
					AAA	-	-	74	0
VS18R	5	Rear Beam Shear Web Panel Between VSS 92 and VSS 111	159	541	40mm	155	109	544	680
					20mm	165	183	698	382
					AAA	-	-	58	0
VS19	5	Rear Beam Fitting at VSS 0	0	-483	40mm	967	-967	483	-1450
					20mm	1740	-2416	1257	-2900
					AAA	-	-	483	-483
VS20	5	Rear Beam Fitting at VSS 0	0	-2848	40mm	911	-911	-1937	-3760
					20mm	1140	-2279	-1709	-5128
					AAA	-	-	-2848	-3408
VS21	5	Rear Beam Cap at VSS 100	0	0	40mm	181	-181	181	-181
					20mm	434	-978	434	-978
					AAA	-	-	362	-724

Table III, Page 2

GAGE	FIGURE REF.	LOCATION	$\Delta\sigma_{LF}$*	$\Delta\sigma_o$	CONDITION	$\Delta\sigma_+$	$\Delta\sigma_-$	$\Delta\sigma_{max}$	$\Delta\sigma_{min}$
AF1	6	FS 990 Frame Bottom at Section A-A	0	188	40mm	491	-415	679	-226
					20mm	679	-1057	868	-868
					AAA	-	-	377	183
AF3	6	FS 990 Frame Middle at Section B-B	0	-183	40mm	367	-256	183	-440
					20mm	367	-917	183	-1100
					AAA	-	-	366	-1100
AF4	7	FS 814 Frame Outside at Section A-A	0	338	40mm	338	-507	677	-169
					20mm	507	-643	846	-304
					AAA	-	-	338	338
AF5	7	FS 814 Frame Top at Section B-b	0	1994	40mm	199	-319	2194	1675
					20mm	399	-479	2393	1516
					AAA	-	-	1994	1396
AF6	8	FS 847 Canted Bulkhead Section A-A	0	-905	40mm	181	-290	-724	-1195
					20mm	362	-362	-543	-1267
					AAA	-	-	-905	-3258
AF7	9	Upper BL 61 Fitting at FS 735 Fwd	0	1321	40mm	226	-377	1547	943
					20mm	377	-679	1698	642
					AAA	-	-	1321	-3962
AF8	10	Upper BL 61 Longeron FS 729 Section Through Bolt 1	0	-71	40mm	285	-357	214	-428
					20mm	178	-357	107	-428
					AAA	-	-	428	-71
AF10	11	Lower BL 61 Fitting FS 744 Aft Section C-C	0	648	40mm	381	-381	1029	267
					20mm	381	-762	1029	-114
					AAA	-	-	648	-2019
AF11	12	Upper BL 61 Longeron FS 992	74	74	40mm	481	-555	555	-481
					20mm	74	-555	148	-481
					AAA	-	-	74	0

Table IV, Page 1

EXPERIMENTAL STRESSES AFT FUSELAGE

GAGE	FIGURE REF.	LOCATION	$\Delta\sigma_{LF}$*	$\Delta\sigma_o$	CONDITION	$\Delta\sigma_+$	$\Delta\sigma_-$	$\Delta\sigma_{max}$	$\Delta\sigma_{min}$
AF12	13	Upper BL 61 Longeron FS 1020	0	37	40mm	733	-550	770	-513
					20mm	367	-587	403	-550
					AAA	-	-	37	37
AF13	14	Upper BL 61 Fitting FS 1039 Section B-B	0	76	40mm	1257	-457	1334	-381
					20mm	381	-648	457	-572
					AAA	-	-	76	-686
AF14	15	Lower BL 61 Fitting FS 1034 Section A-A	0	-912	40mm	365	-365	-547	-1276
					20mm	365	-438	-547	-1350
					AAA	-	-	182	-912
AF15	16	Lower BL 61 Longeron FS 1030	0	807	40mm	293	-550	1100	257
					20mm	293	-550	1100	257
					AAA	-	-	807	-110
AF18	17	Fitting Upper Dorsal Longeron FS 946 Section C-C	0	37	40mm	367	-293	403	-257
					20mm	550	-1284	587	-1247
					AAA	-	-	37	37
AF20R	18	Fuselage Skin . FS 741 . Lower BL 79 . Panel Q	0	670	40mm	98	107	759	571
					20mm	242	933	901	503
					AAA	-	-	168	465
AF21R	18	Fuselage Skin . FS 833 Lower BL 54 Panel K	0	792	40mm	237	242	1049	602
					20mm	307	643	1081	296
					AAA	-	-	89	460
AF22R	18	Fuselage Skin FS 1000 Upper BL 32 Panel C	0	2163	40mm	184	520	2346	2122
					20mm	55	292	1521	2369
					AAA	-	-	78	110
C1	19	40mm Gun Elevation Rod	-	-	40mm	6160	-3697	6160	-3697
					20mm				
					AAA				

Table IV, Page 2

GAGE	FIGURE REF.	LOCATION	$\Delta\sigma_{LF}$*	$\Delta\sigma_{o}$	CONDITION	$\Delta\sigma_{+}$	$\Delta\sigma_{-}$	$\Delta\sigma_{max}$	$\Delta\sigma_{min}$
68	19	40mm Gun Trunnion Rod	-	-	40mm 20mm AAA	1269	-2115	1269	-2115

Table IV, Page 3